Spatial distribution of NF-κB transcriptional activity and expression of pro-inflammatory and cytoprotective proteins in murine aorta

Dissertation for the degree *Cand. Pharm.* **by Gunhild Kile Sandvik**

Cardiovascular Medicine Unit, National Heart and Lung Institute
Imperial College, London

Department of Pharmaceutical Biosciences
School of Pharmacy
Faculty of Mathematics and Natural Sciences
University of Oslo 2007

Table of contents

Table of contents 2
Acknowledgements 4
Abstract 5
Abbreviations 7
1 Introduction 9
1.1 Cardiovascular diseases/ Atherosclerosis 9
1.2 Atherosclerosis and inflammation 10
1.2.1 Atherosclerotic lesion development 10
1.2.2 The arterial endothelial cell 13
1.2.3 Activation of the endothelial cell 14
1.3 Flow and atherosclerosis 15
1.3.1 Mechanotransduction of shear stress 16
1.3.2 Effects of shear stress on endothelium 17
1.4 NF-κB regulates endothelial activation and apoptosis 18
1.4.1 The NF-κB family 19
1.4.2 Activation of NF-κB 19
1.4.3 Biological function of NF-κB 21
Inflammation 21
Cell viability and apoptosis 21
1.4.4 Target genes of NF-κB 22
VCAM-1 22
A1 23
1.4.5 Nrf2 - a potential mediator of the cytoprotective effect of high shear on endothelial cells 23
1.4.6 NF-κB and atherosclerosis 24
1.4.7 Flow, NF-κB and atherosclerosis 25
1.5 Hypotheses 26
1.6 Specific questions to be addressed 26
2 Methods and materials 28
2.1 Animals 28
2.2 In vivo stimulation of aortic endothelium 29
2.3 Ex vivo stimulation of aortic endothelium 29
2.4 Dissection of the aorta to visualize HP ad LP areas of atherosclerotic lesions 30
2.5 Immunohistostaining of the murine aorta en face 31
2.5.1 Antibodies 31
2.6 Confocal laser scanning microscopy 32
2.6.1 The confocal microscope used in this study 33
2.6.2 Excitation of fluorophores and detection of fluorescence 34
2.6.3 Image acquisition 35
2.6.4 Data analysis 36
2.7 Luminescence detection in transgenic reporter mice 36
2.7.1 Low resolution luminescence imaging 37
2.7.2 High resolution luminescence imaging 37
2.7.3 High resolution reflected light imaging 38

2.7.4 Data analysis ... 38
3 Results ... 39
3.1 Correlation between endothelial cell morphology and atherosusceptible and atheroresistant regions in the murine aorta ... 39
3.2 Induction of inflammatory response in vascular endothelium ... 40
3.2.1 Responses of murine aortae to TNF-α treatment *ex vivo* ... 41
3.2.2 LPS stimulation *in vivo* ... 42
3.3 Spatial distribution of NF-κB expression and activities in the murine aorta ... 44
3.3.1 RelA levels in regions protected and susceptible to atherosclerotic lesion formation ... 44
Confirmation of results by co-staining of EC using anti-RelA and anti-CD31 antibodies ... 47
3.3.2 NF-κB transcriptional activity in HP and LP regions of murine aorta ... 48
3.3.3 NF-κB expression and activity at intercostal ostia ... 50
Spatial variation in NF-κB expression levels at intercostal ostia ... 50
NF-κB luciferase activity in aorta at sites of disturbed flow ... 51
3.4 Expression of NF-κB target genes in suscept. and resist. regions of the aorta ... 53
3.4.1 Spatial distribution of VCAM-1 ... 53
3.4.2 Distribution of A1 in the murine aorta ... 54
3.5 Spatial distribution of Nrf2 in areas exposed to disturbed and laminar flow ... 56
3.5.1 Nrf2 expression and activity in atherosusceptible regions of the murine aorta ... 57
3.5.2 Nrf2 luciferase transcriptional activity in the murine aortic endothelium ... 59
4 Discussion ... 61
4.1 Endothelial cell morphology in atherosusceptible and atheroresistant regions in the murine aorta ... 61
4.2 Spatial distribution of NF-κB in the murine aorta ... 62
4.2.1 The NF-κB subunit RelA display increased expression and activity in athero-prone sites of the murine aorta ... 62
4.2.2 NF-κB transcriptional activity is elevated in HP vs LP regions of the murine aorta in response to LPS ... 63
4.2.3 NF-κB activity is elevated in regions of the murine aorta exposed to abnormal hemodynamic flow ... 64
4.3 Expression of selected NF-κB target genes in atherosusceptible and atheroresistant regions of the murine aorta ... 65
4.3.1 EC at atherosusceptible sites are primed for enhanced expression of the pro-inflammatory NF-κB target gene VCAM-1 in response to LPS ... 65
4.3.2 Expression of the cytoprotective protein A1 is upregulated by LPS in the murine aorta ... 66
4.3.3 NF-κB target genes are induced by LPS treatment ... 66
4.4 Does high shear stress mediate atheroprotective effects in aortic endothelium by activating Nrf2 ... 67
4.5 Spatial distrib. of NF-κB activity in the aorta and its relevance in atherosclerosis ... 68
5 Conclusion ... 70
6 References ... 71
Internet references ... 76

Acknowledgements

The work for this dissertation was mainly performed at the Cardiovascular Medicine unit, National Heart and Lung Institute, Imperial College, London.

First and foremost, I would like to thank my supervisor, Dr Paul Evans. He has been a tremendous support, always giving helpful and constructive advice in both major and minor issues regarding my study. I am grateful for guidance in designing experiments and for him generally being an enthusiastic and inspiring supervisor! He is also acknowledged for welcoming me to join him and his colleagues in the Intracellular Signalling group.

I would like to thank my in-house supervisor, Dr Harald Thidemann Johansen for making it possible for me to carry out my study with Dr Evans group.

Parts of my work were performed at the Institute for Nutrition research, University of Oslo. I would like to thank Dr Harald Carlsen for having me in his lab and providing transgenic mice. Thanks to Dr Harald Hauglin for his knowledge and assistance in image acquisition and for support in analyzing my luminescence data.

Thanks to Miss Gabrielle Turner and Miss Jennifer Lucas for introducing me to experimental animal work.

Finally, I would like to thank Karine, Hera, Mustafa, Le and Øyvind for all the fun in and outside of the lab throughout this memorable year!

Oslo, October 2007

Gunhild Kile Sandvik

Abstract

Vascular inflammation and atherosclerosis occur predominantly at branches and bends of arteries that are exposed to complex hemodynamics, whereas straight arteries exposed to unidirectional laminar flow are protected. Recent studies of murine arteries have revealed that complex hemodynamics are associated with enhanced endothelial expression of RelA, a member of the NF-κB family of transcription factors that regulates inflammation and apoptosis by inducing both pro-inflammatory (e.g. VCAM-1) and cytoprotective (e.g. A1) molecules. The distribution of NF-κB/RelA and the expression of NF-κB-dependent proteins in the murine aortic endothelium were evaluated by *en face* antibody staining of aortae followed by confocal microscopy and image analysis.

In C57BL/6 mice, RelA expression was significantly elevated in areas of complex hemodynamics. Also, after lipopolysaccharide treatment, the pro-inflammatory NF-κB dependent protein VCAM-1 and the cytoprotective protein A1 were increased in the endothelium of this area. Furthermore, transgenic luciferase reporter mice revealed that NF-κB transcriptional activity was strongly induced in areas of complex hemodynamics. This suggests that endothelial cells exposed to complex hemodynamics may be primed for enhanced NF-κB activation and induction of pro-inflammatory proteins on encountering activatory stimuli.

The protective effect of laminar flow on arteries may be a result of the activation of antioxidant genes via an Nrf2/EpRE-dependent transcriptional pathway. I examined this idea by assessing the expression levels of Nrf2 and its activity in regions of the murine aorta exposed to either complex or uniform hemodynamics. I observed by immunohistostaining that Nrf2 protein levels were increased in endothelial cells at the atherosusceptible region (exposed to complex flow) compared to the atheroresistant region (exposed to uniform flow). However, these data were not consistent with

subsequent analyses of transgenic mice containing an Nrf2 (EpRE)-luciferase reporter which revealed that Nrf2 transcriptional activities were similar in atherosusceptible and atheroresistant regions. I conclude that although Nrf2 is expressed at elevated levels in atherosusceptible regions of the aorta its transcriptional activity is uniform throughout the aorta. These data do not support the hypothesis that enhanced Nrf2 activities are responsible for protecting arteries exposed to uniform hemodynamics from inflammation.

We conclude that the hemodynamic environment in arteries may have a pivotal role in the expansion and progression of atherosclerotic lesion. My data suggests that NF-κB may be an important determinant of the susceptibility of arteries to inflammation, whereas I did not find evidence for a role for Nrf2. Thus the NF-κB signal transduction pathway could serve as a novel and attractive therapeutic target for the prevention and treatment of atherosclerosis.

Abbreviations

ARE	Antioxidant Response Element
Bcl-2	B-cell leukemia/lymphoma 2
Bfl-1/A1	Bcl-2-Related Protein A1
CCD	Charge Coupled Device
CCR2	(C-C motif) Receptor 2
CD31	Cluster of Differentiation molecule 31
CXCR3	(C-X-C motif) Receptor 3
EC	Endothelial Cell(s)
EpRE	Electrophile-Response Element
FELASA	Federation of European Laboratory Animal Science Associations
GADD45β	Growth Arrest and DNA Damage-inducible 45 Beta
HP	High Probability of atherosclerotic lesion formation
HUVEC	Human Umbilical Vein Endothelial Cells
ICAM-1	Intercellular Adhesion molecule 1
IκB	I kappa B
IKK	I kappa B Kinase
IL-1	Interleukin-1
IL-8	Interleukin-8
ILR	Interleukin Receptor
Keap-1	Kelch-like ECH-associated protein 1
LP	Low Probability of atherosclerotic lesion formation
LPS	Lipopolysaccharide
LSM	Laser Scanning Microscopy

MCP-1	Monocyte Chemoattractant Protein 1
M-CSF	Macrophage Colony-Stimulating Factor
MMPs	Matrix Metalloproteinases
MnSOD	Manganese Superoxide Dismutase
NF-κB	Nuclear Factor kappa B
Nrf2	Nuclear factor erythroid 2-related factor 2
ox-LDL	oxidized Low-Density Lipoprotein
PAMPs	Pathogen-Associated Molecular Patterns
PBS	Phosphate-Buffered Saline
RHD	Rel Homology Domain
ROS	Reactive Oxygen Species
RT	Room Temperature
SLE	Systemic Lupus Erythematosus
TLR	Toll-Like Receptors
TNFα	Tumor Necrosis Factor-alpha
TNFR	Tumor Necrosis Factor Receptor
VCAM-1	Vascular Cell Adhesion Molecule 1
VE-Cadherin	Vascular Endothelial Cadherin
VEGRF2	Vascular Endothelial Growth Factor Receptor 2

1 Introduction

1.1 Cardiovascular diseases/ Atherosclerosis

Cardiovascular disease is the number one cause of death globally and is projected to remain the leading cause of death in the foreseeable future. An estimated 17.5 million people died from this condition in 2005, representing 30 % of all global deaths. The major causes are 'modifiable risk factors' such as tobacco use, physical inactivity and an unhealthy diet (internet reference 1). Atherosclerosis is a progressive condition in which patchy deposits of fatty materials, atheromas, develop in medium sized and large artery walls. This leads to reduced or blocked blood flow in vital organs such as brain, heart and kidneys and is the most important contributor to the growing burden of cardiovascular diseases.

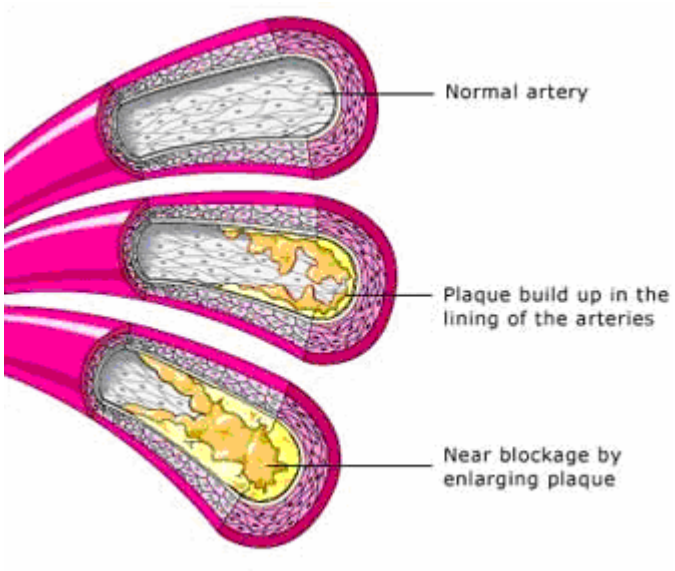

Figure 1.1 Development of atherosclerosis.
Lipid deposition in arteries may lead to blockage of the blood stream and subsequent tissue and organ damage. Image adapted from internet reference 2.

1.2 Atherosclerosis and inflammation

The view of the pathophysiology of atherosclerosis has evolved over the past century. From being a condition in which hyperlipidemia was thought to be the main factor (Ross & Harker, 1976), it is now acknowledged that inflammation has a prominent role in the development of this disease. Recent research has established a fundamental role for inflammation in mediating all stages of this disease, from initiation through progression and ultimately the thrombotic complications (Libby *et al.*, 2002).

The inflammatory response involves three major stages: first, dilation of capillaries to increase blood flow; second, microvascular structural changes and escape of plasma proteins from the bloodstream; and third, leukocyte transmigration through endothelium and accumulation at the site of injury. The main focus here will be on the latter stage.

1.2.1 Atherosclerotic lesion development

Early atherosclerotic lesions (fatty streaks) contain monocytes and T lymphocytes which are recruited from the circulation by adhesion to activated vascular endothelial cells (EC). The normal endothelium does not usually support binding of white blood cells; however undergoing inflammatory activation, arterial EC increases expression of selective adhesion molecules on their surface. In several steps, which all are equally important for the inflammation reaction, these adhesion molecules bind to leukocytes through cognate ligands. Selectins mediate a rolling interaction with the inflamed luminal endothelium, whilst other adhesion proteins mediate firmer attachment and eventually transmigration of the adherent leukocyte and finally accumulation in the intima. In particular, the immunoglobulin-like vascular cell adhesion molecule 1 (VCAM-1) plays a major role in leukocyte attachment by binding both monocytes and T-lymphocytes upon endothelial activation (Huo & Ley, 2001). The leukocyte transmigration requires a chemoattractant gradient. Various chemokines participates in this process,

monocyte chemoattractant protein 1(MCP-1) with its receptor CCR2 (Gu *et al.,* 1998) and interferon-γ -inducible chemokines with their receptor CXCR3 (Mach *et al.*, 1999).

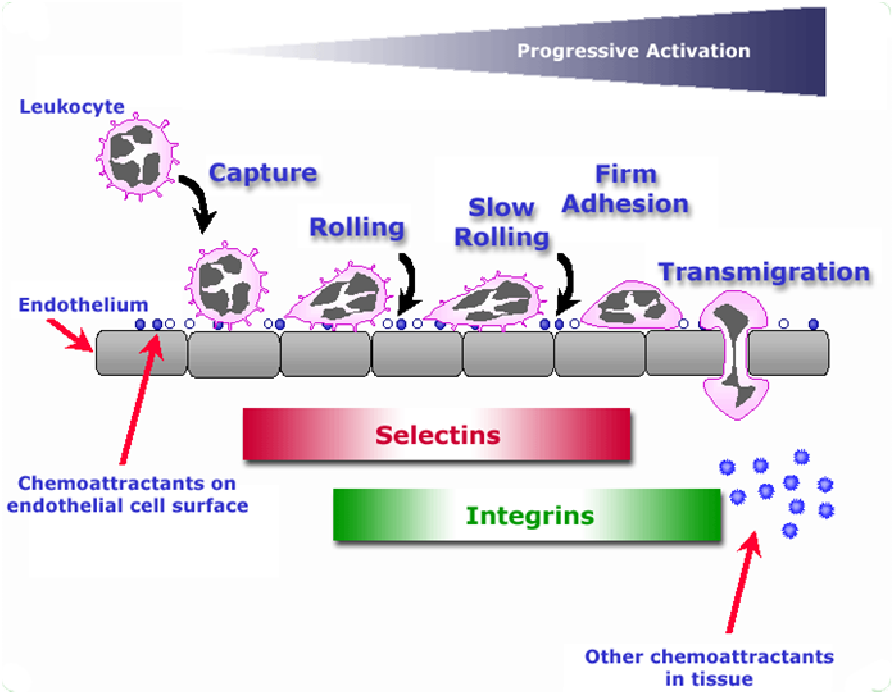

Figure 1.2 Leukocyte transmigration upon stimulation of the inflammatory system.
Upon endothelial activation leukocytes are accumulated in the intima through several steps. Image adapted from internet reference 3.

In the presence of oxidized low density lipoproteins (ox-LDL), accumulated monocytes are converted to macrophages upon activation by macrophage colony-stimulating factor (M-CSF) among others (Clinton *et al.,* 1992). By increased expression of scavenger receptors, the macrophages ingest modified lipoprotein particles such as cholesteryl esters which accumulate in cytoplasmic droplets. This leads them to differentiate into arterial foam cells which assemble in a central core in the typical atherosclerotic plaque. Notably, foam cells secrete reactive oxygen species (ROS) and pro-inflammatory cytokines such as MCP-1 which can amplify the local inflammatory response in the lesion. They also produce matrix metalloproteinases (MMPs) which in turn can lead to destabilization and

consequently rupture of the plaque's fibrous cap. This will lead to contact of the blood with another macrophage product called tissue factor which is a potent pro-coagulant protein. Consequently, this can advance the pathophysiology of cardiovascular disease by leading to thrombosis and obstruction of blood flow throughout the circulatory system.

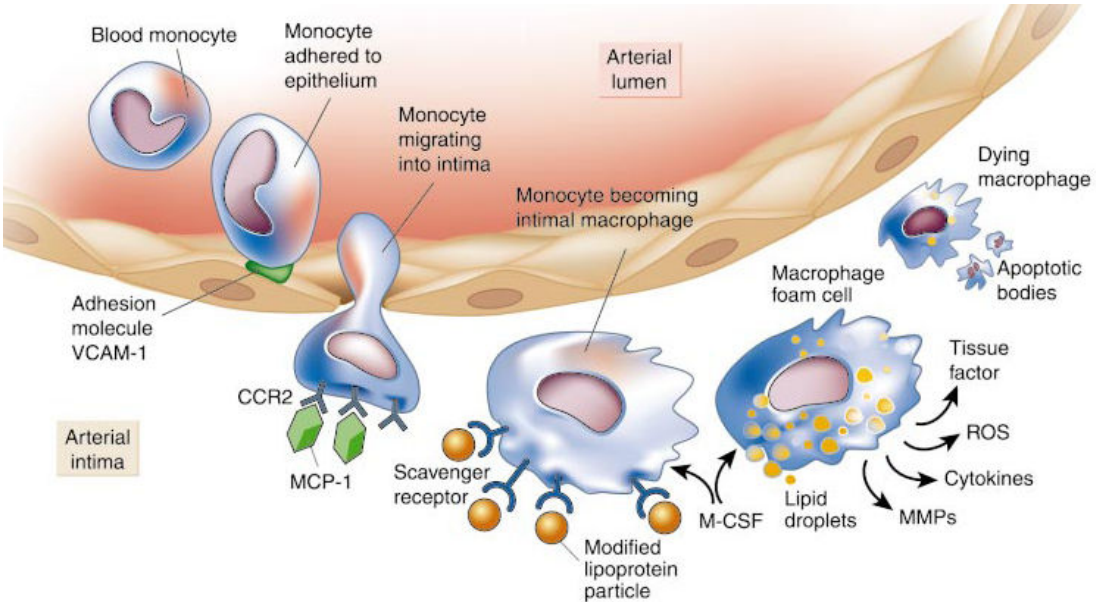

Figure 1.3 The role of the monocyte in lesion development.
The formation of arterial foam cells is initiated by monocyte adhesion to the endothelium. Image adapted from (Libby, 2002).

Transmigrated T-lymphocytes are also activated upon encounter with antigen such as ox-LDL and heat shock proteins. Crosstalk between these leukocytes and macrophages amplifies pro-inflammatory cytokine, MMPs and tissue factor release. Together with resident vascular wall cells, T-lymphocytes secrete cytokines and growth factors that can promote the migration and proliferation of smooth muscle cells. These may express specialized enzymes that can degrade the extracellular matrix of the growing plaque, leaving the fibrous cap weak and susceptible to rupture (Libby *et al.*, 2002).

After formation of the fatty streak, the emerging atheroma typically evolves into a more complex lesion, which eventually may lead to clinical manifestations.

1.2.2 The arterial endothelial cell

The arterial endothelium survives remarkably well as the interface between blood and the vessel wall in an environment of constantly changing biomechanical stresses as well as acute and chronic exposure to inflammatory stimulants (e.g. cytokines and hypercholesterolemia respectively) (Davies, 2007).

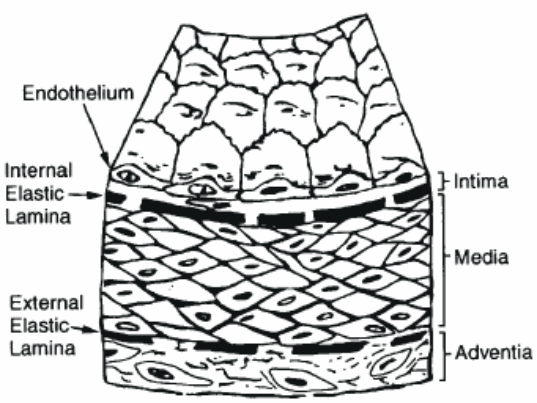

Figure 1.4 The endothelium.
Endothelial cells line the blood vessel wall. Image obtained from internet reference 4.

Endothelial cells are key regulators of the inflammatory response in the vascular system. Lining blood vessels, they provide in the steady state an anti-inflammatory, anti-coagulatory surface. However, in the case of injury or infection, EC control the adhesion and migration of blood leukocytes, as well as the fluid exchange from the blood stream to the damaged tissue. Thus, expression of endothelial adhesion molecules, cytokines and fluid exchange needs to be tightly regulated to allow for a controlled inflammatory response (Kadl & Leitinger, 2005).

1.2.3 Activation of the endothelial cell

Several factors are known to activate EC including microbial products which may be circulating due to intercurrent infections. For instance, lipopolysaccharide (LPS) from the cell wall of *Escherichia coli,* is known to activate EC through Toll-like receptor 4 (TLR4) (Netea *et al.,* 2002). In addition pro-inflammatory cytokines such as tumor necrosis factor alpha (TNFα) and interleukin-1 (IL-1) may be locally produced and/or circulating due to inflammatory comorbidity (e.g. systemic lupus erythematosus (SLE), rheumatoid arthritis) and activate the endothelium (Haskard, 2004*).* Thus microbial products, TNFα, IL-1 and other factors activate EC, leading to increased expression of adhesion molecules and cytokine production which enhances recruitment and activation of leukocytes. (Kol & Libby, 1998). Signalling through receptors of the TNF, IL-1 or TLR families proceeds via distinct pathways that converge to activate the inhibitory κB kinases (IKK) which phosphorylate inhibitory κB (IκB) (Hayden & Ghosh, 2004). The phosphorylated form is then destabilized, thus releasing free nuclear factor kappa B (NF-κB) for nuclear translocation and stimulation of transcription.

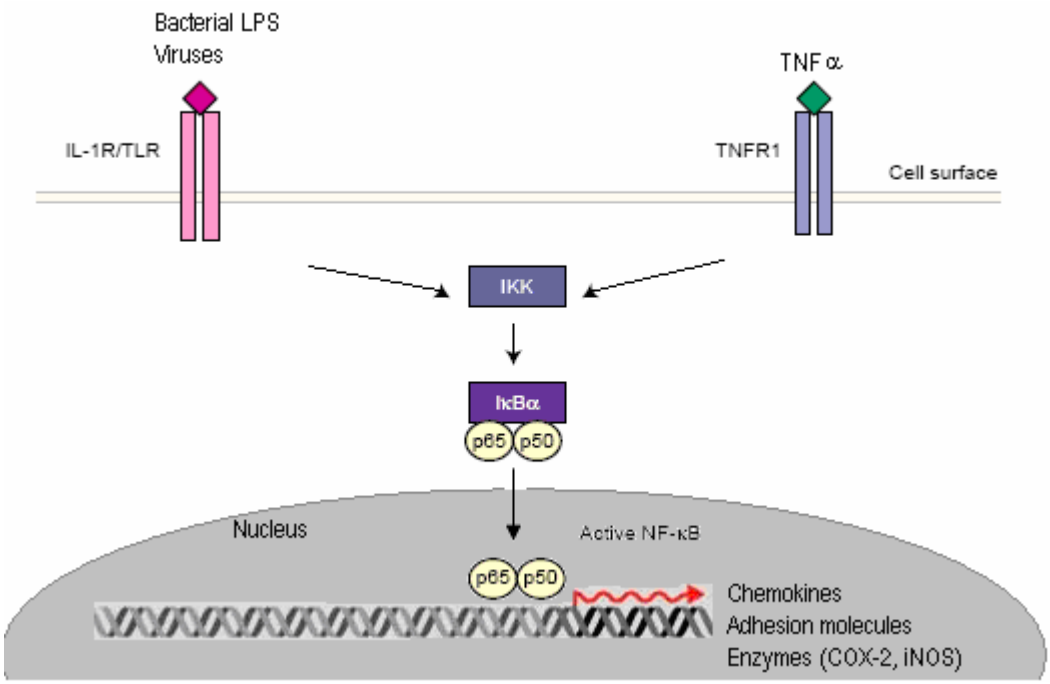

Figure 1.5 Activation of the NF-κB pathway through TLR and TNFR1.
A schematic and simplified representation of the NF-κB activation. Image adapted from (Evans, 2005), modified.

1.3 Flow and atherosclerosis

Atherosclerosis is a geometrically focal disease that has a predilection to branches, bifurcations and bends of the arterial tree. In these susceptible areas, blood flow is slow and oscillatory, resulting in a low hemodynamic shear stress at the endothelium. In contrast, straight vessel segments experience pulsatile, unidirectional laminar flow which induces a high average of shear stress on the endothelium. High shear stress is associated with the absence of atherosclerosis, even when plasma risk factors such as hypercholesterolemia are present (Zarins *et al.,* 1983).

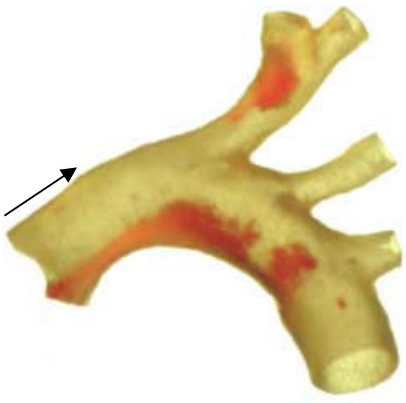

Figure 1.6 Formation of atherosclerotic plaque at the aortic arch.
Blood flow assumes a disturbed or turbulent pattern. Red patchy distribution indicates areas of low shear and lipid deposition. Arrow indicates direction of blood flow. Aortic arch from original by G. García-Cardeña.

Shear stress is a biomechanical force expressed in units of dynes/cm^2 that is determined by blood pressure, vessel geometry and fluid viscosity (Resnick *et al.,* 2003). Thus, the endothelium is exposed to diverse flow patterns; unidirectional laminar flow which promotes high shear stress and disturbed, oscillatory flow which expose the EC to low shear.

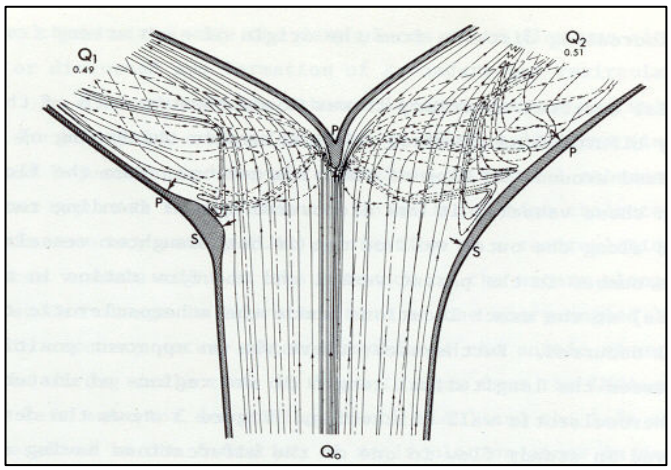

Figure 1.7 Flow patterns in the ascending and descending aorta.
This figure shows the aorta opened to visualize the lumenal side. The upper part corresponds with the aortic arch which experiences disturbed flow, while the lower part is the descending aorta with laminar flow. Image adapted from (Motomiya & Karino, 1984).

1.3.1 Mechanotransduction of shear stress

There appears to be several possible mechanisms by which EC can sense stress and act as a shear transducer.

Endothelial cells are specifically equipped with a dedicated sensing mechanism to detect shear stress. The mechanical force is amplified by shear deformation of specialized cellular mechanotransduction elements of the cytoskeleton. Furthermore, the cytoskeleton is coupled to the cellular membrane in a distributed manner by elements that include integrins, cell-cell adhesion molecules and receptors. Conformational changes of the specific proteins of these connecting complexes lead to an activation of intracellular signalling molecules, which then leads to transcriptional activity of target genes. For example, it has recently been demonstrated that unidirectional laminar shear can be sensed through a CD31/ VE-Cadherin/ VEGFR2 tri-molecular complex that converts mechanical force into biochemical signals (Tzima *et al.,* 2005).

Primary cilium has been described for epithelial cells in the renal, bile and pancreatic duct. (Bisgrove *et al.*, 2006; Satir *et al.,* 2007). Recently, primary cilia have also been demonstrated on endothelial cells, especially in regions of low and disturbed hemodynamic flow. (Iomini *et al.,* 2004; Van der Heiden *et al.,* 2006). It has been suggested that primary cilia elevate the shear responsiveness of endothelial cells to prevent atherogenic activation, but little is still know about this possible mechanism.

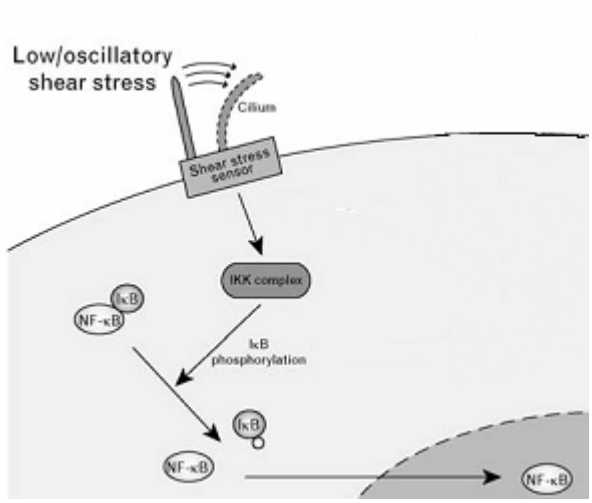

Figure 1.8 Possible mechanism regarding sensing of low shear stress by endothelial cells.
The endothelial cell is activated upon low/oscillatory shear stress. Image obtained from (Helderman *et al.,* 2007), modified.

1.3.2 Effects of shear stress on endothelium

Regions exposed to low and oscillatory shear stress conditions are pro-thrombotic, pro-migratory, pro-apoptotic and correlate well with the localization of atherosclerotic lesions. The arterial endothelium in these regions is activated and demonstrates increased uptake of lipoproteins, lipid deposition, increased surface expression of leukocyte adhesion molecules and leukocyte transmigration. All these factors correspond with early signs of fatty streaks and lesion formation (Malek *et al.,* 1999; Traub & Berk, 1998). The EC display heterogeneity in response to disturbed flow and undergo transformation of cell morphology. They obtain polygonal cell shapes and a random orientation that reflect the local

hemodynamic conditions. The EC also appear to be at a higher density in low shear regions (Hajra *et al.,* 2000).

In contrast to the potentially harmful effects of low shear stress, high rates of unidirectional laminar flow is generally vasoprotective and associated with anti-thrombotic, anti-migration and pro-survival effects. (Malek *et al*., 1999; Traub & Berk 1998). The EC appear elongated, homogenic and tightly aligned to the direction of blood flow (Hajra *et al.,* 2000). Prolonged high shear exerts several 'atheroprotective' effects on EC, including inhibition of the cell cycle (Lin *et al.,* 2000), suppression of thrombosis (Grabowski *et al.,* 2001) and promotion of viability (Jin *et al*., 2002; Taba *et al.,* 2003; Dimmeler *et al.,* 1996; Dimmeler *et al.,* 1998; Dimmeler *et al.,* 1999; Hermann *et al.,* 1997). Several lines of evidence suggest that chronic high shear also suppresses inflammation. As an example, EC adhesion molecules are expressed at reduced levels at atheroprotected sites of the vasculature exposed to high shear (Hajra *et al.,* 2000; Iiyama *et al.,* 1999). Also, prolonged high shear can suppress the induction of adhesion molecules by pro-inflammatory cytokines in perfused aortae (Yamawaki *et al.,* 2003) or in cultured EC (Dai *et al.,* 2004; Sheikh *et al.,* 2003; Sheikh *et al.,* 2005; Chiu *et al.,* 2004).

1.4 NF-κB regulates endothelial activation and apoptosis

NF-κB is a transcription factor that regulates the transcription of a large number of genes, particularly those involved in inflammatory, acute stress and survival responses. Through interaction with specific inhibitory proteins, the IκBs, NF-κB is retained in the cytoplasm in an inactive state. Proteolytic degradation of IκB that has been phosphorylated by IKK, liberates NF-κB to enter the nucleus and activates NF-κB regulated target genes. This process is eventually terminated through NF-κB-induced synthesis of IκBs and, consecutively, cytoplasmic resequestration of this transcription factor (Senftleben & Karin, 2002).

1.4.1 The NF-κB family

In mammals, the NF-κB family consists of five members: NF-κB1 (p105/p52), NF-κB2 (p52/p100), RelA (p65), RelB and c-rel. In unstimulated cells, these family members exist as homo- or heterodimers bound to IκB family proteins. Heterodimers composed of p50/RelA are the most abundant form of NF-κB in most cell types including EC. Characteristic of the NF-κB proteins are the conserved 300 amino acid Rel homology domain (RHD) that is located towards the N terminus. This domain is responsible for dimerization, interaction with IκBs, and binding to DNA (Hayden & Ghosh, 2004).

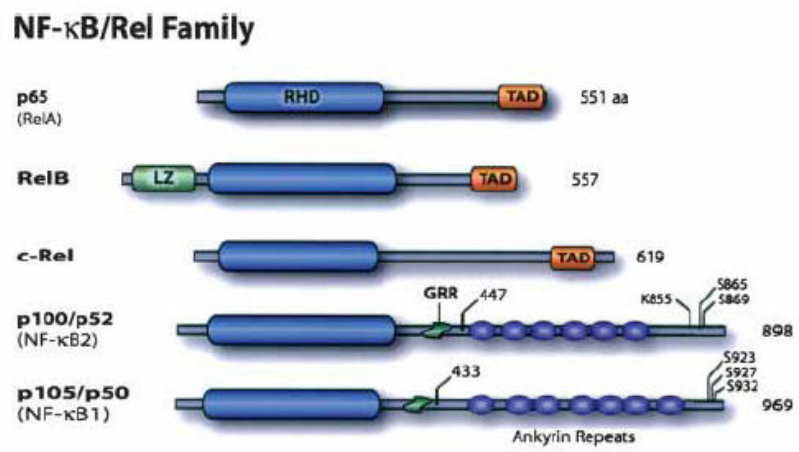

Figure 1.9 Schematic representation of NF-κB family of proteins.
Image obtained from (Hayden & Ghosh, 2004).

1.4.2 Activation of NF-κB

Two major signalling pathways lead to translocation of NF-κB dimers from the cytoplasm to the nucleus; the classical pathway, which is of most importance for this project, and the alternative pathway. In the classical pathway, pro-inflammatory cytokines and pathogen-associated molecular patterns (PAMPs) cause activation of the β-subunit of the IKK complex (complex consisting of the IKKα and IKKβ catalytic subunit and the IKKγ regulatory subunit, see Figure 1.10). This activation is implemented through receptors belonging to the TNFR and TLR/IL-1R superfamilies. The activated IKK complex catalyzes the

phosphorylation of IκBs on two N-terminal serine residues, which are then polyubiquitinated, targeting them for degradation by the proteosome. The released NF-κB dimer translocates to the nucleus, where it binds to sequences in promoter or enhancer regions of target genes and thereafter activate transcription. Signalling via this pathway results in a rapid activation of IKK and nearly complete degradation of IκBα within 10 min.

In the alternative pathway, the homodimer IKKα is activated and phosphorylates p100 which is subsequently cleaved to generate a 52kD fragment that functions as the p52 NF-κB sub-unit.

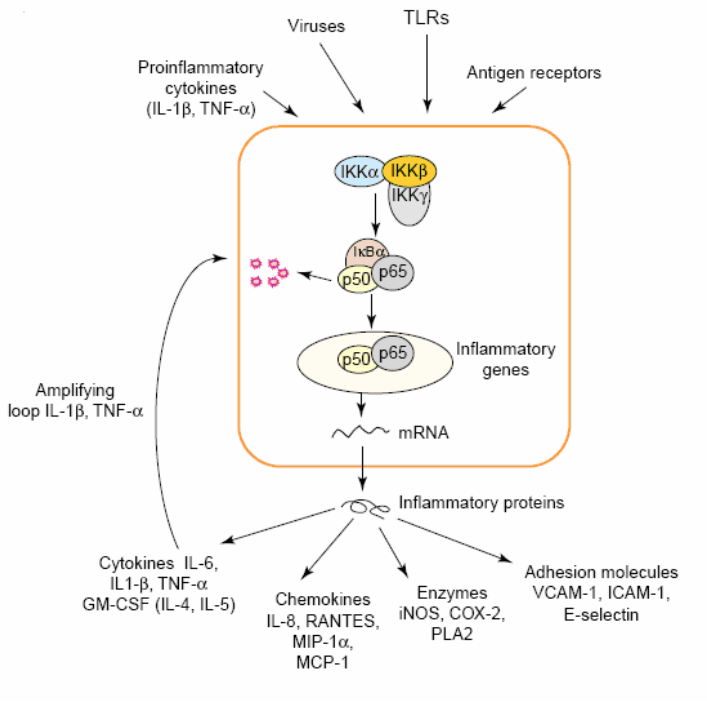

Figure 1.10 The classical NF-κB activation pathway.
This pathway is activated by a variety of inflammatory signals, resulting in coordinate expression of multiple inflammatory and innate immune genes. The pro-inflammatory cytokines IL-1β and TNFα is induced in response to NF-κB activation, thus forming an amplifying feed forward loop. Image obtained from (Bonizzi & Karin, 2004).

1.4.3 Biological function of NF-κB

NF-κB activates various target genes that is important to the pathophysiology of the vessel wall, including cytokines, chemokines and leukocyte adhesion molecules, as well as genes that regulate cell proliferation and mediate cell survival (see Figure 1.10). In addition, the IκBα gene is also activated, thus increasing the cytoplasmic pool of the NF-κB inhibitor. This autoregulatory system ensures that the induction of NF-κB is transient and that the activated cell eventually goes back to a quiescent state (Collins & Cybulsky, 2001).

Inflammation

It is widely established that the classical NF-κB pathway based on IKKβ-dependent IκB degradation is essential for innate immunity. For example, RelA and IKKβ deficiencies result in an increase in susceptibility to infections (Alcamo *et al.*, 2001). The activation of NF-κB dimers, preferably the p50/RelA dimer, leads to the transcription of genes encoding several mediators important for the innate immune response to infection and injury. Notably, chemokines, cytokines, adhesion molecules (ICAM-1, VCAM-1 and E-selectin), enzymes that produce secondary inflammatory mediators and inhibitors of apoptosis (Ghosh *et al.,* 1998).

Cell viability and apoptosis

Programmed cell death is a highly regulated process initiated by the absence of survival factors or presence of death-promoting factors. All cells contain components of the death machinery, ready to initiate self-destruction unless signalled not to do so. Cells undergoing apoptosis shrink and retract from neighbouring cells, this is followed by condensation of the chromatin at the nucleus membrane, whilst other organelles appear normal.

Endothelial cell apoptosis or dysfunction (loss of vasomotor tone, alteration in pro-coagulant activity and inflammation) is of great importance in many diseases, including atherosclerosis. In the diseased tissue, additional factors present (such as inflammatory cytokines) substantially alter the balance of cell proliferation and apoptosis to varying degrees. Specific alterations within the cell itself are also involved in the regulation of this balance (Stoneman & Bennett, 2004). Evidence supports a pro-active role for NF-κB in the inhibition of cell death induced by TNFα and other death causing agents (Van Antwerp *et al.,* 1998). Interestingly, the p50/RelA heterodimer governs EC viability through the activation of cytoprotective genes, including Bcl-2, A1, GADD45β and MnSOD (DeSmaele *et al.,* 2001; Duriez *et al.,* 2000; Wong *et al.,* 1989).

1.4.4 Target genes of NF-κB

VCAM-1

VCAM-1 is an immunoglobulin-like adhesion molecule that can be induced in endothelial cells exposed to pro-inflammatory stimuli including LPS, TNFα and ox-LDL. Similarly, *in vivo* studies indicate that VCAM-1 can be rapidly induced by atherogenic conditions in rabbits, mice and humans (Huo & Ley, 2001). There is abundant evidence that NF-κB is required for VCAM-1 expression in activated EC. Firstly, the VCAM-1 promoter contains NF-κB-binding elements. Secondly, studies of cultured EC revealed that VCAM-1 expression can be inhibited by inhibitors of NF-κB (Collins & Cybulsky, 2001). Finally, VCAM-1 expression is suppressed in transgenic mice that express an IκB 'superrepressor' that blocks NF-κB activity in vascular endothelium (Henke *et al.*, 2007).

Once expressed on the surface of EC, VCAM-1 binds to the integrin a4b1 which is constitutively expressed on lymphocytes, monocytes and eosinophils, and induces both rolling-type adhesion and firm adhesion upon encounter. It is structurally similar to ICAM-1 and other endothelial adhesion molecules,

but has a unique distinct pattern of regulation (Huoy & Ley, 2001). Its role in atheroclerosis has been thoroughly demonstrated (Nakashima *et al.,* 1998; Cybulsky *et al.,* 2001; O'Brien *et al.,* 1993). For example, by transient blocking of VCAM-1 adhesion pathways by antibodies or peptides in LDLR -/- mice fed a high fat diet, a reduced monocyte and lipid accumulation in lesions were obtained (Huo & Ley, 2001).

A1

B-cell leukemia/lymphoma 2 (Bcl-2) is a family of intracellular membrane proteins that localizes to mitochondria, endoplasmic reticulum and the nuclear envelope (Monaghan *et al.,* 1992). Bcl2 proteins have been shown to block apoptosis without inducing cellular proliferation (Hockenbery *et al.,* 1990). The pro-survival Bcl-2 homologue Bfl-1/A1 is a direct transcriptional target of NF-κB. A1 can be induced by TNFα in EC and it plays an essential role in protecting TNFα-treated EC from apoptosis (Duriez *et* al., 2000). Studies of A1 in immune tissues and cells support the concept that NF-κB exerts cytoprotective effects by inducing A1 (Zong *et al.,* 1999).

1.4.5 Nrf2 - a potential mediator of the cytoprotective effect of high shear on endothelial cells

Oxidative signals play a significant role in the pathogenesis of chronic inflammatory diseases by mediating expression of inflammatory genes. However, the protective mechanisms of antioxidant systems remain poorly defined. The Nrf2/EpRE pathway may serve as an endogenous antioxidant system within the vasculature that is activated by atheroprotective laminar flow. The electrophilic response element (EpRE; otherwise known as the antioxidant response element (ARE)) is a transcriptional regulatory element that mediates expression of a set of antioxidant proteins. NF-E2-related factor 2 (Nrf2) is a transcription factor that is responsible for both constitutive and inducible expression of the EpRE-regulated genes. In endothelial cells, the EpRE-mediated genes are

upregulated by laminar shear stress through an Nrf2-dependent mechanism. Under basal conditions, Nrf2 resides mainly in the cytoplasm bound to its cystein-rich, Kelch domain-containing partner, Keap1. On exposure to electrophile or oxidative stresses, Nrf2 is liberated from Keap1-dependent repression and accumulates in the nucleus to regulate the induction of a family of antioxidant genes (Kobayashi & Yamamoto, 2005). This suggests that Nrf2 contributes to the anti-atherosclerotic response via the EpRE. Nrf2 has been shown to play a part in the regulation of inflammation in both EC and macrophages (Hosoya *et al.,* 2005; Chen *et al.,* 2005). Interestingly, in EC, the over-expression of Nrf2 inhibits the TNFα-mediated activation of the VCAM-1 promoter (Chen *et al.,* 2003). Consistent with these findings, it has also been shown that Nrf2 gene-knockout mice develop an autoimmune-like disease characterised by inflammation of multiple organs (Chen & Kunsch, 2004).

1.4.6 NF-κB and atherosclerosis

Using monoclonal antibodies that recognize the IκB binding region on the RelA subunit, activated NF-κB has been identified *in situ* in human atherosclerotic plaques. It has also been revealed that very little activated NF-κB is present in healthy vessels. In models of arterial injury, NF-κB is activated in both endothelial and smooth muscle cells. In healthy arteries, p50 and RelA seem to have a diffuse expression that is restricted to the cytoplasm of EC and smooth muscle cells. However, within human atheromas, NF-κB sub-units accumulate in the nucleus of both cell types suggesting that the transcription factor is activated (Brand *et al.,* 1996). Activated NF-κB has also been detected in intimal cells found in coronary arteries of pigs fed a hypercholesterolemic diet (Wilson *et al.,* 2000). Collectively, these observations support a role for NF-κB in atherosclerosis.

As earlier described, multiple genes whose products are thought to be involved in the atherosclerosis process are regulated by NF-κB. This involves both induction of genes that stimulate recruitment of

circulating monocytes, leukocyte transmigration and smooth muscle cell migration and proliferation. As a result of this activation, cytokine and chemokine release and growth factor production can be mediated. We can therefore conclude that NF-κB may be the key to both initial responses to the atherogenic signal and to subsequent amplification steps during the outspread and advancement of atherosclerotic lesions (Collins & Cybulsky, 2001).

1.4.7 Flow, NF-κB and atherosclerosis

The molecular mechanism underlying the anti-inflammatory and cytoprotective effects of shear stress on EC is uncertain. Preliminary data from the intracellular signalling group by Dr Paul Evans revealed that:

1. Prolonged high shear modulates responses of cultured endothelial cells to the atherogenic cytokine TNFα by suppressing subsequent induction of pro-inflammatory transcripts including E-selectin, VCAM-1 and IL-8. In contrast to the effects of shear on pro-inflammatory transcripts, it was revealed that prolonged high shear primes EC for enhanced expression of NF-κB-dependent cytoprotective molecules such as Bcl-2, A1, MnSOD and GADD45β in response to TNFα. (Partridge *et al.,* 2007)

2. In addition, preliminary studies of NF-κB-luciferase reporter mice suggested that NF-κB transcriptional activity was strongly induced in EC at the aortic arch by LPS whereas activity in the descending aorta was relatively weak. (Partridge *et al.,* 2007)

Studies by Myron Cybulsky's group have revealed that EC exposed to relatively low shear at the lesser curvature of the aorta contain high levels of the RelA NF-κB sub-unit and are primed for pro-inflammatory (e.g. VCAM-1) induction in response to LPS. (Hajra *et al.,* 2000)

My study of the relationship between flow in murine arteries and pro-inflammatory activation will improve our understanding of the molecular mechanisms that govern the spatial distribution of atherosclerotic plaques. It is conceivable that findings from the proposed study may inform new therapeutic strategies to suppress inflammation at atherosusceptible regions by targeting NF-κB.

1.5 Hypotheses

We hypothesise that expression and activities of NF-κB transcription factors are regulated by shear stress in vascular endothelium *in vivo*. Specifically, we predict that EC exposed to low or oscillatory shear will be primed for enhanced NF-κB activation and expression of pro-inflammatory proteins in response to pro-inflammatory stimuli e.g. LPS. In contrast, we predict that NF-κB-dependent pro-inflammatory activation will be suppressed in EC exposed to high levels of unidirectional, laminar shear. We also hypothesise that the activity of Nrf2 may be enhanced in vascular endothelium exposed to high shear region, and that this transcription factor may play a role in atheroprotection.

1.6 Specific questions to be addressed

In this project I examined whether NF-κB activation and expression of pro-inflammatory molecules in murine vascular endothelium were *correlated* with shear stress. Thus I compared endothelial activation in the greater curvature of the aortic arch (exposed to high unidirectional shear) with endothelial activation in the lesser curvature (exposed to low oscillatory shear). I also studied the ostia (branching points) of the intercostal arteries which are regions exposed to abnormal hemodynamics and low oscillatory shear.

The following specific questions were addressed:

1. Do *expression levels* of RelA NF-κB sub-units in EC vary between the greater and lesser curvatures of the aortic arch and branch points of the great vessels?

2. Do NF-κB *transcriptional activities* in EC vary between the greater and lesser curvatures of the aortic arch and branch points of the great vessels? If so, do regions of high NF-κB activity correspond to regions of high RelA NF-κB protein levels?

3. Do the expression patterns of VCAM-1 differ between greater and lesser curvatures and if so, do they correspond to the pattern of NF-κB transcriptional activity?

4. Does the expression pattern of A1 differ from VCAM-1?

5. Do *expression levels* and activities of Nrf2 in EC vary between the greater and lesser curvatures of the aortic arch and branch points of the great vessels?

2 Materials and methods

2.1 Animals

C57BL/6 is a common inbred mouse strain and is one of the most widely used strains in the study of atherosclerosis and in the development of mutant mouse lines. This mouse strain was used throughout my immunofluorescence staining experiments. Male mice supplied from Harlan Olac Ltd were sacrificed at 8-12 weeks of age (20-25g).

For some of my preliminary experiments a BXSB1,4 mouse strain was used. This was allowed optimisation of technical aspects of the work to be performed using excess animals that were available in the department and due to be euthanized. This recombinant inbred strain is a model for chronic inflammation; they are prone to the disease SLE. The mice were used at different ages and both sexes.

To investigate the activity of particular transcription factors I used transgenic mice that were developed by Dr Harald Carlsen and Prof Rune Blomhoff at the Institute of Nutrition Research, University of Oslo.

To assess NF-κB transcriptional activity in the murine aorta, transgenic mice that express a luciferase reporter whose transcription is dependent upon NF-κB (3x-κB-luc) were used. 3x-κB-luc male heterozygous mice with (C57BL/6) genetic background were sacrificed at the age of 24 weeks.

A strain which reports on ARE/EpRE was used to investigate constitutive Nrf2 activity in the murine aorta. Female mice with (C57BL/6 x CBA) genetic bakcground were sacrificed at 40 weeks of age.

All experiments were performed within guidelines set by the Federation of European Laboratory Animal Science Association (FELASA).

2.2 *In vivo* stimulation of aortic endothelium

Systemic administration of LPS from gram negative bacteria wall triggers the activation of the immune system through the induction of cytokine release

I administered varying doses of LPS from *Escherichia coli* serotype 055:B5 (Sigma) which were diluted to a volume of 0.5 ml in phosphate-buffered saline (PBS, GIBCO) before slowly injecting it into the peritoneal cavity of the mouse. The duration of effect before fixation of the aortic endothelium was adjusted to ensure maximum expression of the protein of interest (30 minutes to 6 hours).

2.3 *Ex vivo* stimulation of aortic endothelium

TNFα is a major mediator of inflammation. For the experiment presented in this thesis, we used a carrier-free TNFα as a stimulus to induce an inflammatory effect in the murine aorta *ex vivo.*

After CO_2-euthanization of the mouse, the unfixed aorta was harvested, cleaned and opened to expose the endothelium. The tissue was then incubated at 37°C in cell culture medium containing 10 ng/ml TNFα (carrierfree, R&D systems) for 30 minutes. An aorta to serve as a control was treated the same way, only without the TNFα. The aortae were then fixed by immersing in formalin (2%, VWR) for approximately 5-10 minutes.

2.4 Dissection of the aorta to visualize high and low probability areas of atherosclerotic lesions

Animals were CO_2 euthanized before the abdomen and ribs were opened longitudinally to expose the thoracic cavity. The right atrium was punctured prior to gentle pressure perfusion by slowly injecting 20 ml PBS through the left ventricle of the heart. The tissue was then pressure fixed with 20 ml formalin (2%, VWR) through the same route. The heart, spleen, one kidney and a part of the liver were snap-frozen in embedding mould (CellPath) at -80º and kept for future use. The aorta and surrounding tissue were carefully harvested from the cadaver and stored in ice cold PBS, before thoroughly removal of perivascular fat. The aortic arch was cut to expose HP and LP regions *en face* as shown in Figure 2.1.

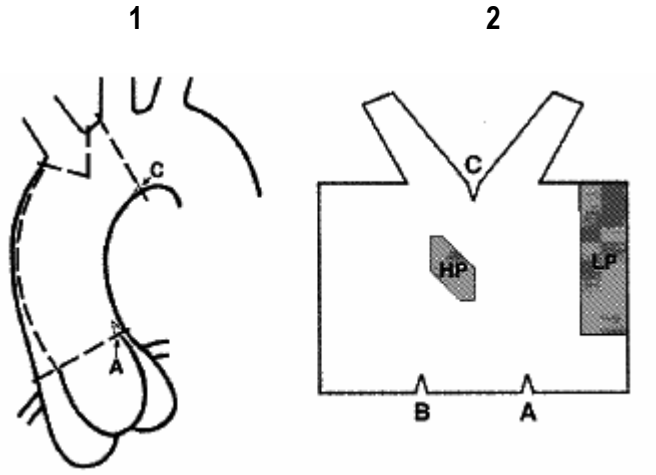

Figure 2.1 Dissection and mapping of HP and LP region for atherosclerotic lesion formation in mice.
(1) The aortic arch is shown with blood stream originating from the bottom (heart not shown). Dashed lines indicate cuts made when dissecting the ascending aorta. (2) *En face* view of HP and LP regions. Small notches at the commissures of the aortic valve (a and b) and at the midpoint of the lesser curvature (c) served as anatomical landmarks. Image obtained from (Iiyama *et al.,* 1999).

The descending aorta was cut in two pieces, one to investigate intercostal ostia the other to serve as a negative control for the secondary antibody.

2.5 Immunohistostaining of the murine aorta *en face*

The tissue was washed in PBS 1-3 times for 5 minutes between each antibody. Blocking and washing steps were performed in a 96-well plate, whilst all immunostaining were performed on a microscope slide covered in parafilm.

The tissue was blocked and permeabilized in 200 μl 20% normal serum (goat serum, DAKO) and 0.5 % Triton-x (Sigma) in PBS overnight at room temperature (RT) (serum used depending on origin of species of secondary antibody). The tissue was then incubated with 100 μl primary antibody solution for 2 hours at RT, or overnight at 4°C. The aortae were incubated in 100 μl fluorescent secondary antibody solution (AlexaFluor®, Invitrogen, diluted 1:1000) with 2% mouse serum (DAKO) for 2 hours at RT in the dark. Where applicable, the tissue was stained with 100 μl endothelial marker solution overnight at RT in the dark. Finally, the samples were stained with nuclear dye (diluted 1:1000) for 30 minutes (To-Pro3, Invitrogen) or 5 minutes (DRAQ-5, Biostatus).

The aortae were put down *en face* onto microscope slides and mounted using non-fluorescing aqueous mounting medium (AquaPolymount, Polysciences). The slides were cover slipped, dried and pressed flat under approximately 3 kg overnight. The tissue was stored at 4°C in the dark and viewed within one week.

2.5.1 Antibodies

Primary antibodies were used as shown in table 2.1.

Table 2.1 Primary antibodies

Primary antibody	Dilution factor
NFκB p65 [sc-372] rabbit (Santa Cruz Biotechnology)	1:200
VCAM-1 [M/K 2.7] rat (Generated from a hybridoma cell line available in the Cardiovascular Sciences Unit)	1:200
A1 [EP517Y] rabbit (AbCam)	1:200
Nrf2 [H-300:sc13032] rabbit (Santa Cruz Biotechnology)	1:100
AlexaFluor® 488 rat αmouse-CD31 [MEC13.3] (BioLegend)	1:100

AlexaFluor® secondary antibodies were used to label the proteins of interest with fluorescence.

2.6 Confocal laser scanning microscopy

Confocal laser scanning microscopy (LSM) is a method that has several advantages over conventional microscope techniques. It creates a sharp image which is achieved by excluding most of the light from the specimen that is not from the focal plan of the microscope. Unwanted light coming from other specimen areas is focused outside the pinhole, which passes only a small fraction of it. The pinhole diameter determines the thickness of the optical section. By increasing the pinhole diameter/optical section the out of focus regions is also increased. The smaller the pinhole, the less stray light or fluorescence from out-of-focus areas will hit the detector. The image will obtain increased resolution and contrast and represents a thin cross-section of the specimen. This method also has the ability to collect serial optical sections taken from the vertical axis of a thick specimen and then rearrange them back into three dimensional projections.

2.6.1 The confocal microscope used in this study

A Zeiss LSM 510 META was used for fluorescent image acquisition. The LSM 5 software, Version 3.2, was used to display and analyze the images, as well as to control the microscope, scanning and laser modules.

Figure 2.2 The confocal microscope.
The Zeiss LSM 510 Meta (image obtained from internet reference 5).

The confocal microscope works by focusing a laser light onto the specimen through an objective in a diffraction-limited mode. Light emitted at the focal plane and at planes below and above it is directed via an XY scanner onto a main dichroic beam splitter, which separates the emissions from the excitation light. The fluorescences are separated from each other by a series of dichroic beam splitters and directed to individual photomultipliers. Separately in each of the channels, the diameters of the pinholes and their XY positions can be optimized, and the desired emission filter placed into the beam path.

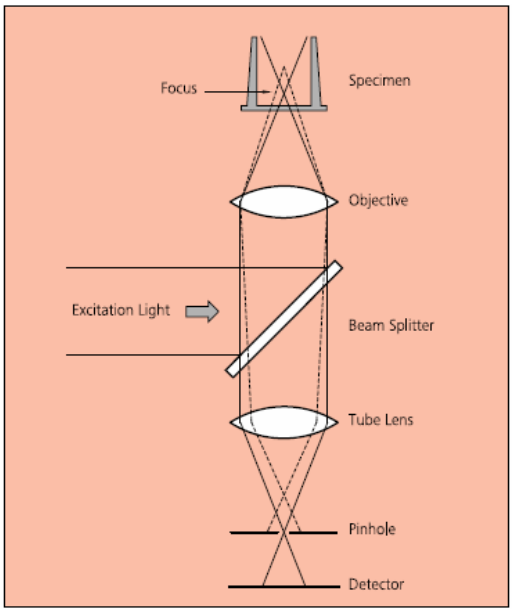

Figure 2.3 Basic setup of a confocal microscope.
Light from the laser is scanned across the specimen by a beam splitter (dichromatic mirror). Optical sectioning occurs as the light passes through a pinhole on its way to the detector (image obtained from internet reference 5).

2.6.2 Excitation of fluorophores and detection of fluorescence

By applying dyes (fluorophores) to specimens, fluorescence can be stimulated and imaged. Fluorescence is emitted when the fluorophore interacts with an incident photon (excitation). Absorption of the photon causes an electron in the fluorophore to rise from its ground state to a higher energy level. Then, the electron reverts to its original level, releasing a photon (fluorescence emission) whose wavelength depends upon the amount of energy that is released during reversion. When the emitted photon has less energy than the absorbed photon, the energy difference is know as Stokes shift.

It is also possible to use more than one type of fluorophore. Thus, by switching the excitation light, different fluorphores can be distinguished in a single specimen. Figure 2.4 shows the absorption and emission spectra of the fluorophores used for the experiments presented in this dissertation. AlexaFluor® dyes were used for their high stability and resistance to photobleaching.

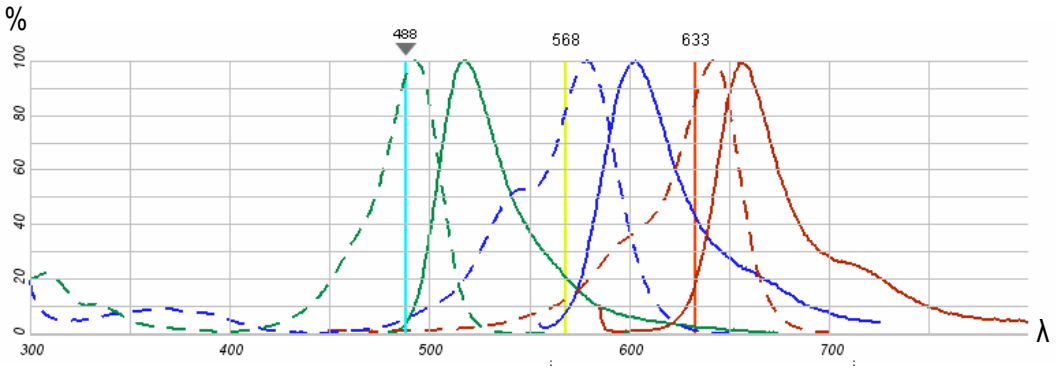

Figure 2.4 Fluorescence spectra.
Absorption (dotted line) and fluorescence emission spectra of AlexaFluor® -488 antibody conjugate (green), AlexaFluor® -568 antibody conjugate (blue), and To-Pro3 (far red) (image obtained from internet reference 6).

2.6.3 Image acquisition

A mercury lamp was used to visualize fluorescence down the microscope to situate the specimen in the right position for optimal imaging. Lasers featuring the appropriate wavelength to excite the dyes used to label the specimen were chosen (Helium-Neon laser 543 nm, 633 nm and Argon ion laser 488 nm)

To remove signal from unspecific staining, a secondary only control was imaged. The level of background was reduced to zero using the amplifier offset. The setting for the channel which through the protein of interest was found was kept constant throughout all the images.

The pinhole was set to 1 Airy Unit to allow detector gain setting and to provide sufficient image information. The detector gain was adjusted to maximum image contrast and brightness for all channels (except the channel of the protein of interest). By manual focusing, the microscope was set to the plane of endothelium with the highest protein signal. A 40/1.3 Oil Plan-Neofluar objective was used. The image resolution was set to 1024x1024 frame scan. Number of averages was set to 8 (mean) to improve signal/noise dramatically. Laser excitation intensity was set to a minimum to reduce level of photo bleaching.

2.6.4 Data analysis

Fluorescent staining was quantified in histograms that illustrate the mean pixel intensity per area. This was measured using the histogram function in the Zeiss LSM 5 software. Areas were chosen by manually defining an area whereas the software calculated the mean intensity inside the area. An example of manually defined areas for quantitation is shown in Figure 2.5.

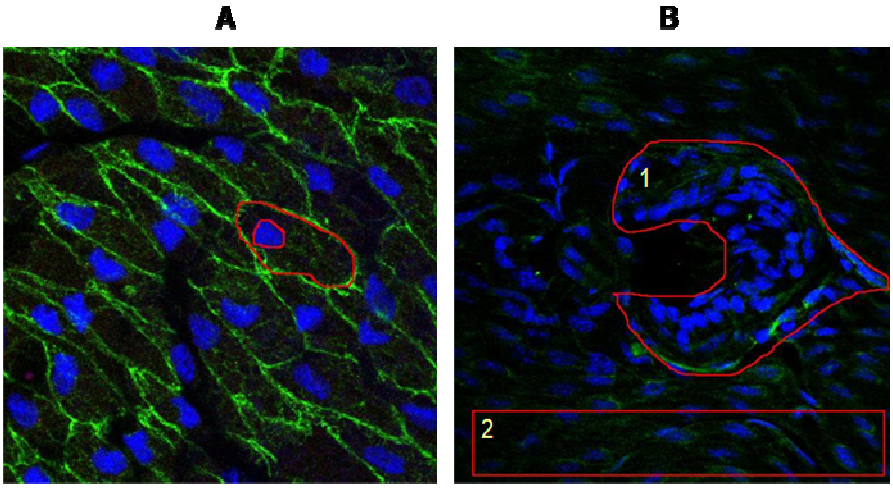

Figure 2.5 Quantitation of fluorescence intensity at endothelium and branching points of vessels.
(A) Two rings were drawn on the image, one following the endothelial/junctional marker (green), and the other following the nuclei marker (blue). (B) One ring was drawn around the intimal cushion (1), whilst an adjacent area served as the control (2).

2.7 Luminescence detection in transgenic reporter mice

The activity of particular transcription factors was determined in luciferase reporter mice by measuring light generation from samples after the administration of luciferin substrate. Some mice were treated with LPS prior to sacrifice whereas other remained untreated. Aortae were carefully harvested from freshly sacrificed transgenic luciferase mice. The tissue was thoroughly cleaned of external fat and aortae were opened longitudinally along the lesser curvature to visualize the endothelium. All manipulations were performed in culture medium to maintain cell viability. The aortae were then immersed *en face* in cell culture medium containing 1.5 mg/ml D-luciferin substrate (Biosynth, Staad, Switzerland).

2.7.1 Low resolution luminescence imaging

Prior to high resolution luminescence imaging, the samples were screened for luciferase activity using the IVIS 100 system from Xenogen. This was useful in determining the exposure length for the high resolution imaging (which could be increased in the case of low luminescence). Software used for image acquisition was Living Image 2.20 from Xenogen.

2.7.2 High resolution luminescence imaging

The macro imaging system used was Andor iXon+ EMCCD camera (DU897E-CSO-#BV) 512x512 pixels, back-illuminated CCD with on-chip electron multiplication. Software used for image acquisition was Andor Solis. Luminescence images were acquired using a Schneider-Kreuznach Xenon 25 mm f/0.95 lens at full aperture opening. A 15 mm extension tube was fitted between the lens and the CCD camera, in order to increase optical magnification and light collection efficiency.

The charge coupled device (CCD) chip was cooled to -100°C with a thermo-electric element, which in turn was water-cooled. Deep cooling of the CCD ensures that false signal due to thermal events (dark current) is negligible. In addition, the effective read-noise was reduced to below one photon per pixel by using on chip electron multiplication with a high gain.

Camera settings for luminescence imaging were:

Exposure time 30 minutes (typically an accumulated image of 6 x 5 minutes)

EMCCD gain 200

16 bit 1 MHz a/D read-out

CCD temperature -100ºC

2.7.3 High resolution reflected light imaging

To obtain high resolution reflected light images, a stereo microscope was used (Leica MZ Apo with a Planapo 1.0x objective 100 W fibre-coupled tungsten lamp used for epi-, trans- and dark-field illumination).

Despite its higher resolution and optical quality, the stereomicroscope was not used for luminescence imaging, due to poorer light gathering power - estimated to be 10% of that of the Schneider lens with extension tube.

2.7.4 Data analysis

Luminescence was analyzed and measured using ImageJ software version 1.37v.

3 Results

3.1 Correlation between endothelial cell morphology and atherosusceptible and atheroresistant regions in the murine aorta

As earlier described, regional differences in hemodynamic flow in the aorta are associated with either protection or susceptibility of formation of atherosclerotic lesions. Areas exposed to disturbed flow have a higher probability of lesion formation (HP), whereas areas exposed to laminar flow are protected and have a low probability of lesion formation (LP). The location of lesion development is highly reproducible, particularly in the ascending aorta and arch. The HP area is located in the lesser curvature and the LP area in the greater curvature of the aortic arch.

Previous studies have shown that EC morphology reflects the local hemodynamic environment (Hajra *et al.,* 2000). The first aim of my project was to identify HP and LP regions in the mouse aorta and validate them by defining EC morphology.

Immunostaining for CD31 (a marker for EC) followed by confocal microscopy showed that EC in the LP region were elongated and organized in a parallel pattern to the direction of blood flow (Figure 3.1, right panel). On the other hand, EC in the HP region possessed polygonal, irregular shapes and were randomly oriented relative to flow direction (Figure 3.1, left panel). The morphology of endothelial nuclei also correlated with the flow pattern in these areas and appeared to be oval and organized in the LP area, where in HP areas they were less organized (Fig 3.1, compare right and left panel).

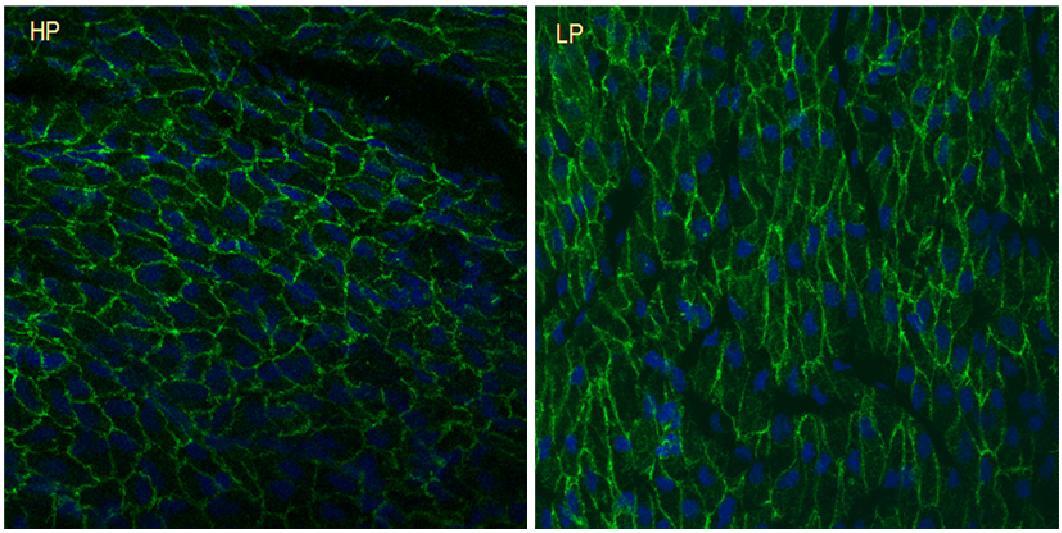

Figure 3.1 The morphology of endothelial cells in HP and LP regions of the murine aorta.
Aorta from an untreated BXSB 1,4 mouse was harvested, fixed and stained *en face* using 488 labelled anti-CD31 antibody (green). Nuclei were counterstained using 633-labelled To-Pro3 (blue). Fluorescence at the lumenal surface of HP and LP sites of the aortic arch was detected using confocal LSM. Note that EC in the HP region have variable shapes and random orientation, whereas in the LP region they are elongated and aligned in the direction of blood flow (top to bottom).

3.2 Induction of inflammatory response in vascular endothelium

I examined whether there were differences in the susceptibility of EC in HP and LP regions to the proinflammatory effects of stimuli such as TNFα and LPS. Although the atherogenic contribution of acute activation is uncertain, inflammatory mediators produced by both acute and chronic infections are thought to modulate the development of atherosclerotic lesions. In the first instance, I studied NF-κB which is known to be activated through exposure of cells to cytokines, chemokines, viruses and bacterial lipopolysaccharides (LPS) among other things and to drive the inflammatory response. To assess the degree of NF-κB activation, we used immunofluorescence staining and confocal microscopy to monitor the nuclear translocation of the NF-κB subunit RelA.

3.2.1 Responses of murine aortae to TNF-α treatment *ex vivo*

TNFα is a pro-inflammatory cytokine which through TNFR1 activation may elicit NF-κB-dependent pathways. To assess its function in murine aortic EC, aortae were harvested and treated with TNFα before fixation and immunostaining.

In untreated vessels, I observed that RelA was predominantly cytoplasmic in EC in both HP and LP regions (Figure 3.2, panels 1-6). Treatment with TNFα led to nuclear localisation of RelA in approximately 50% of the EC in both HP and LP regions (Figure 3.2, panels 7-12).

By comparison with the effects of TNFα on cultured EC which induces RelA nuclear localization in all cells (Partridge *et al*., 2007), we were surprised at the inconsistent response of murine aortic EC to TNFα applied *ex vivo*. The unequal response of EC in this experiment may be due to mechanical forces imposed on the EC during the process of dissection and cleaning of the aorta, which may have altered their physiology

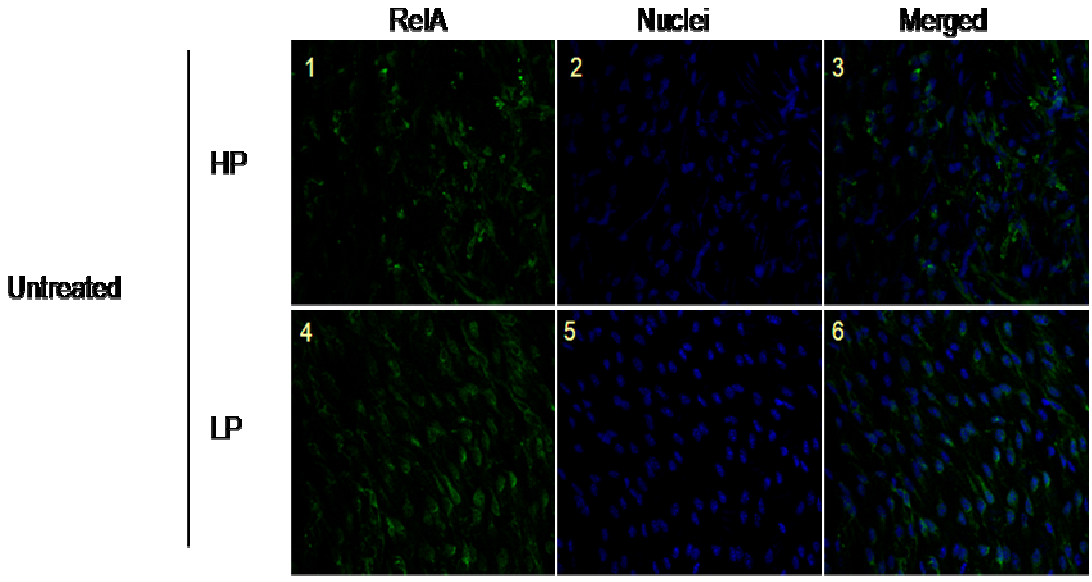

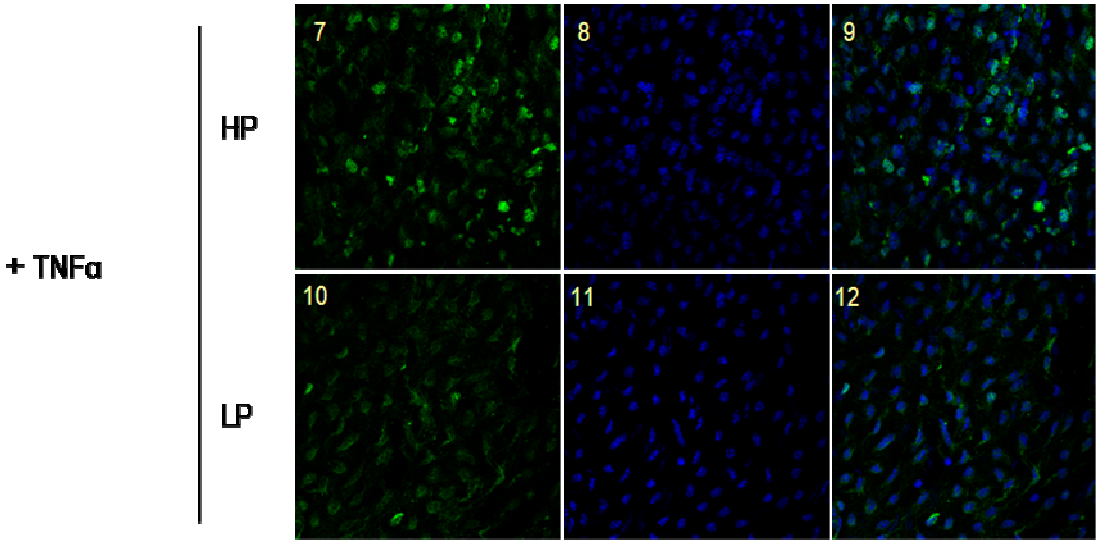

Figure 3.2 Induction of inflammatory response in vascular endothelium *ex vivo.*
Aortae from untreated BXSB 1,4 mice were harvested and incubated at 37°C in medium for 30 min (Panels 1-6) or 10 ng/ml TNFα in medium for 30 min (Panels 7-12) (n=1 in each group). Aortae were then fixed and stained *en face* using anti-RelA primary antibodies and AlexaFluor 488-conjugated secondary antibodies (green). Nuclei were counterstained using 633-labelled To-Pro3 (blue). Fluorescence at the lumenal surface of HP and LP sites of the aortic arch was detected using confocal LSM. Note that EC in both HP and LP areas show an incomplete translocation of RelA from the cytosol to the nucleus in response to TNFα.

3.2.2 LPS stimulation *in vivo*

As stimulation did not induce a complete translocation of RelA from the cytosol to the nucleus in EC *ex vivo*, we decided to administer a pro-inflammatory stimulus *in vivo.* We chose to use LPS instead of TNFα because LPS has generated more reliable and consistent pro-inflammatory activation *in vivo* in our experience (Partridge *et al*., 2007). Other investigators have shown that administrating 100 µg (5 mg/kg) LPS to the intraperitoneal cavity gives an acute systemic activation of vascular endothelium (Hajra *et al*., 2000). In the first instance I examined the effects of varying doses of LPS (50 µg or 100 µg) on NF-κB nuclear translocation in aortic EC.

Immunostaining showed that 50 µg and 100 µg LPS provoked a translocation of RelA from the cytosol to the nucleus in both HP and LP regions of the murine aorta. Figure 3.3 show that RelA was detected exclusively in the nucleus of EC of treated animals and I concluded that a dose of 50 µg LPS is sufficient for an acute systemic activation.

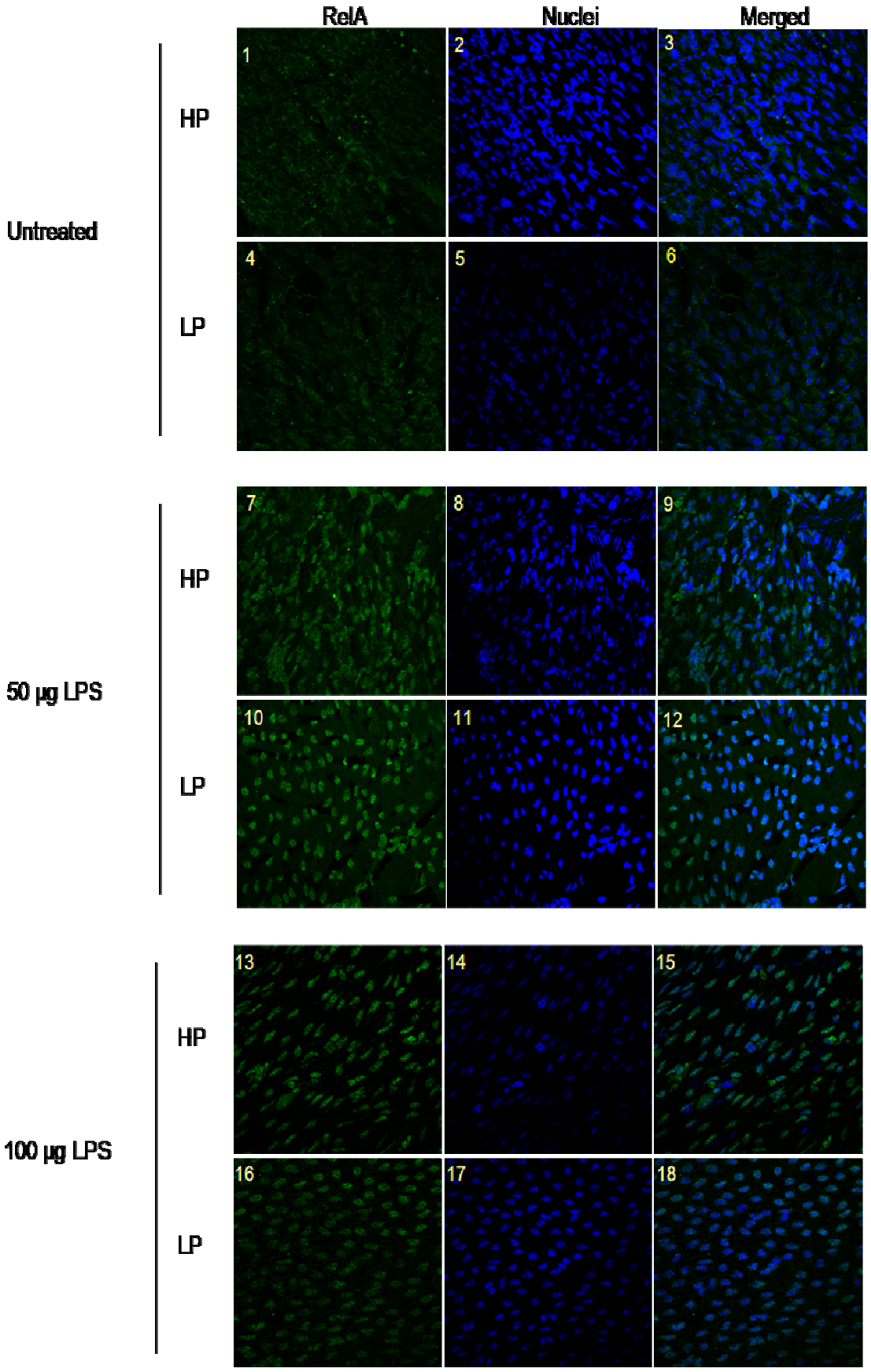
RelA
Nuclei
Merged
Untreated
HP
LP
50 µg LPS
HP
LP
100 µg LPS
HP
LP
1
2
3
4
5
6
7
8
9
10
11
12
13
14
15
16
17
18

Fig 3.3 Induction of inflammatory response in vascular endothelium *in vivo.*
BXSB 1,4 mice were treated with 0, 50 or 100 µg LPS i.p. for 30 min (n=2). Aortae were harvested, fixed and stained *en face* using anti-RelA primary antibodies and AlexaFluor 488-labelled secondary antibodies (green). Nuclei were counterstained using 633-labelled To-Pro3 (blue). Fluorescence at the lumenal surface of HP and LP sites of the aortic arch was detected using confocal LSM. Representative images of HP and LP regions obtained from the same mouse are shown. Note that doses of both 50 and 100 µg LPS (panels 7-18) induce a translocation of RelA from the cytosol to the nucleus in both HP and LP sites compared to the control (panels 1-6).

3.3 Spatial distribution of NF-κB expression and activities in the murine aorta

Previous data from the Intracellular Signalling group have shown that shear stress and TNFα alters the intracellular localization of RelA in human umbilical vein endothelial cells (HUVEC). It has also been shown that EC in the aortic arch of transgenic NF-κB luciferase reporter mice were primed for enhanced NF-κB activation in response to TNFα (Partridge *et al.,* 2007). To validate and extend these data, I looked at the distribution of the RelA subunit as well as NF-κB luciferase activity in EC *in vivo*.

3.3.1 RelA levels in regions protected and susceptible to atherosclerotic lesion formation

Immunostaining and confocal microscopy revealed that RelA protein levels are significantly elevated in the HP region compared to the LP region (Figure 3.4 A, compare panels 1 and 4; Figure 3.4 B, upper panels). The proportion of RelA in the nucleus versus the cytosol is also significantly increased in the HP region (in the absence of LPS) (Figure 3.4 A, panel 1-3; Figure 3.4 B, panel 3). These data suggest that the HP area may be primed for pro-inflammatory activation. Upon acute systemic stimulation of the immune system via LPS injection, RelA translocated to the nucleus in both HP and LP regions (Figure 3.4 A, 7-12; Figure 3.4C, panels 2 and 4). The extent of NF-κB translocation in response to LPS was similar in both regions as assessed by quantitation of RelA in nuclear or cytoplasmic regions (Figure 3.4 B, panel 4) or by examining co-localization of RelA with a nuclear marker (Figure 3.4 C).

A

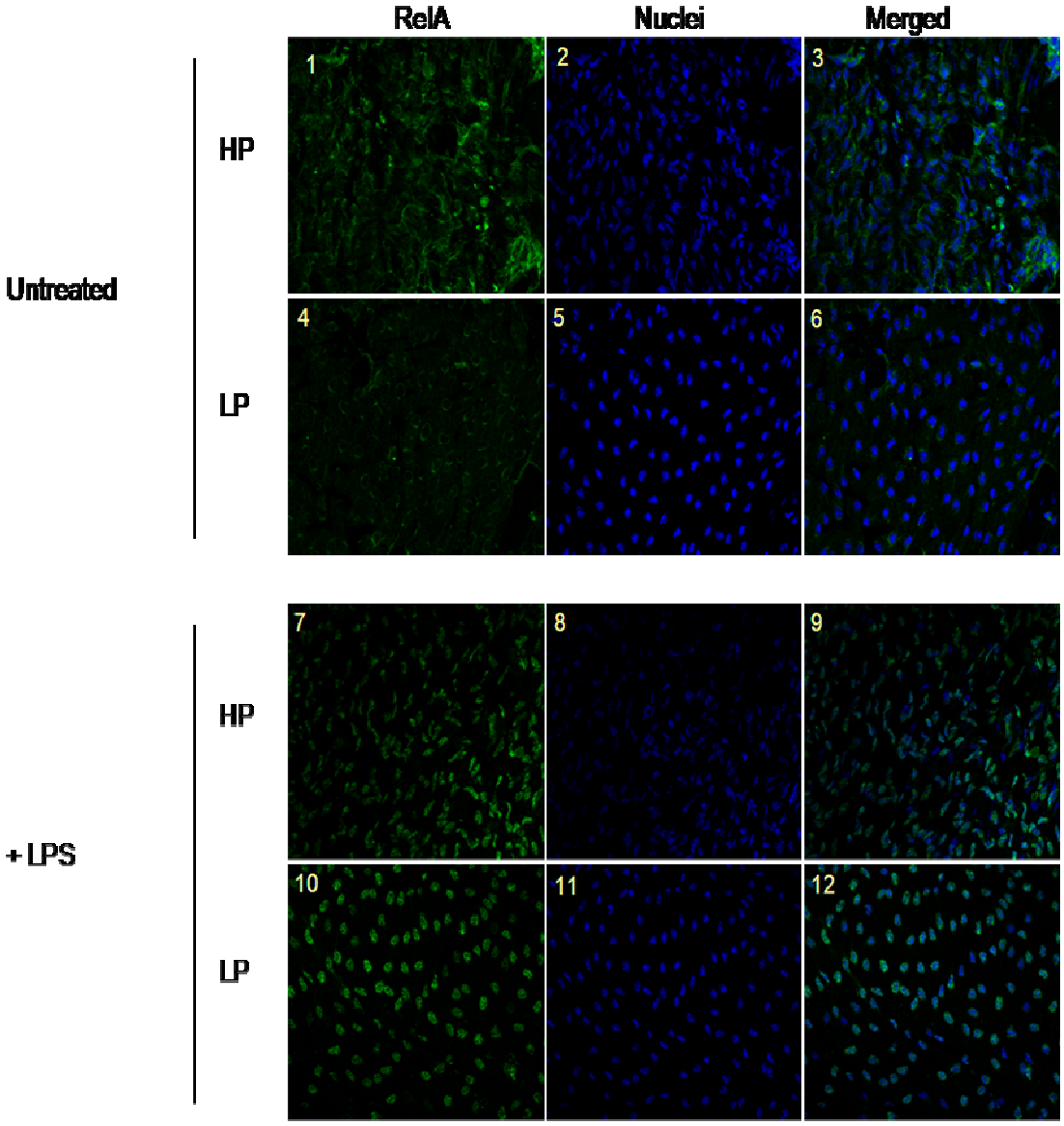
RelA
Nuclei
Merged
Untreated
HP
LP
+ LPS
HP
LP
1
2
3
4
5
6
7
8
9
10
11
12

B

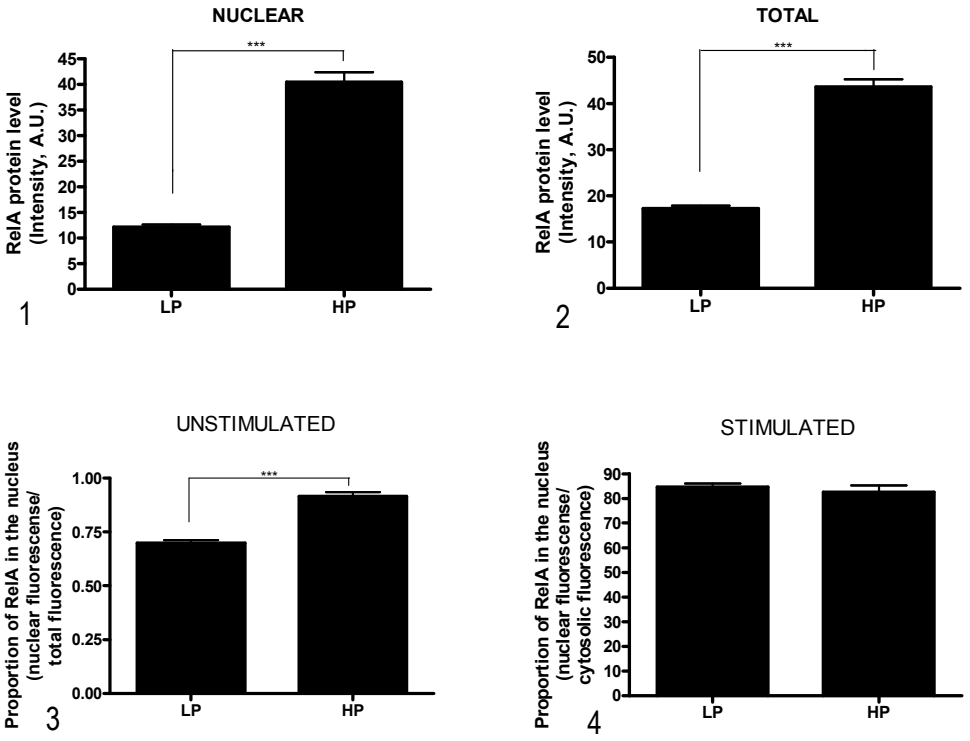
NUCLEAR
RelA protein level (Intensity, A.U.)
***
LP
HP
1
TOTAL
RelA protein level (Intensity, A.U.)
***
LP
HP
2
UNSTIMULATED
Proportion of RelA in the nucleus (nuclear fluorescense/ total fluorescence)
***
LP
HP
3
STIMULATED
Proportion of RelA in the nucleus (nuclear fluorescense/ cytosolic fluorescence)
LP
HP
4

C

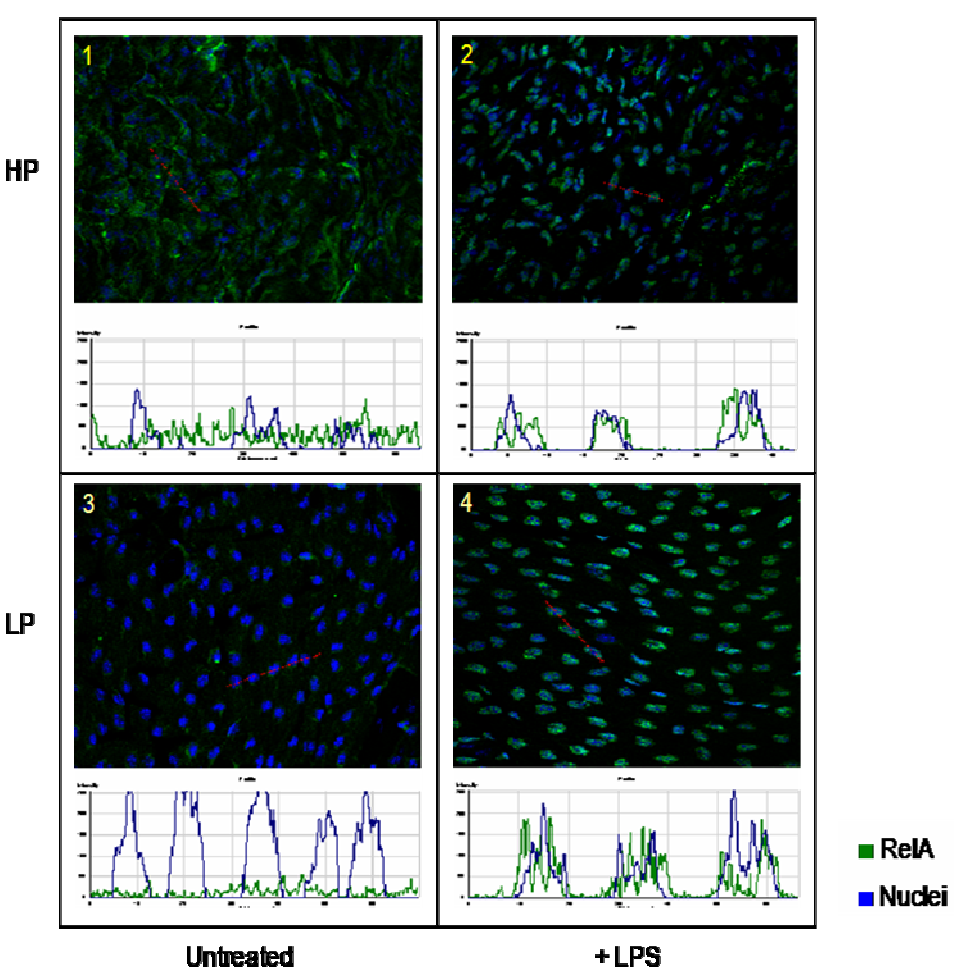
HP
LP
1
2
3
4
RelA
Nuclei
Untreated
+LPS

Fig 3.4 The spatial distribution of RelA in the murine aortic arch
(A) C57BL/6 mice were injected with 50 µg LPS i.p. for 30 minutes (panels 7-12) or remained untreated as controls (panels 1-6) (n=4 in each group). Aortae were fixed and then stained *en face* using anti-RelA primary antibodies and AlexaFluor 488-conjugated secondary antibodies (green). Nuclei were counterstained using 633-labelled To-Pro3 (blue). Fluorescence at the lumenal surface of HP and LP sites of the aortic arch was detected using confocal LSM. Representative images of HP and LP regions obtained from the same mouse are shown. (B) Fluorescence was quantified in 100-150 cells randomly selected from 5-10 images of each area. RelA levels were quantified in whole cells (TOTAL) or in nuclei (NUCLEAR) of EC from untreated animals (upper panels). The ratio of nuclear: cytoplasmic RelA, which is a measure of NF-κB activation, was calculated for EC of untreated or treated animals (lower panels). Data are shown as means ±SEM (arbitrary units, A.U.). Differences between samples were analyzed using a paired t-test (***$p<0.0001$). (C) NF-κB nuclear localisation was also examined by determining the extent of co-localization of RelA and To-Pro3 by measuring fluorescence intensity through cross sections of 3-5 cells for each image. The position of the cross sections was chosen manually and is represented as a red line in the images (upper panels). Fluorescence intensities through cross sections were plotted (lower panels). Note the co-localisation of RelA and nuclei in EC at HP or LP sites of LPS-treated animals, indicating that RelA translocates to the nucleus in response to LPS in both regions.

Confirmation of results by co-staining of EC using anti-RelA and anti-CD31 antibodies

In the previous section I identified EC using confocal microscopy by focusing on the lumenal side of the aorta and by reference to anatomical details, including nuclear morphology. However, to confirm that RelA expression levels are elevated in *endothelial cells* at HP sites we performed co-staining using anti-RelA and anti-CD31 (an endothelial marker) antibodies. These findings (Figure 3.5) show conclusively that RelA is found to lesser extent in LP regions than HP regions in untreated endothelium, thereby confirming our previous analysis.

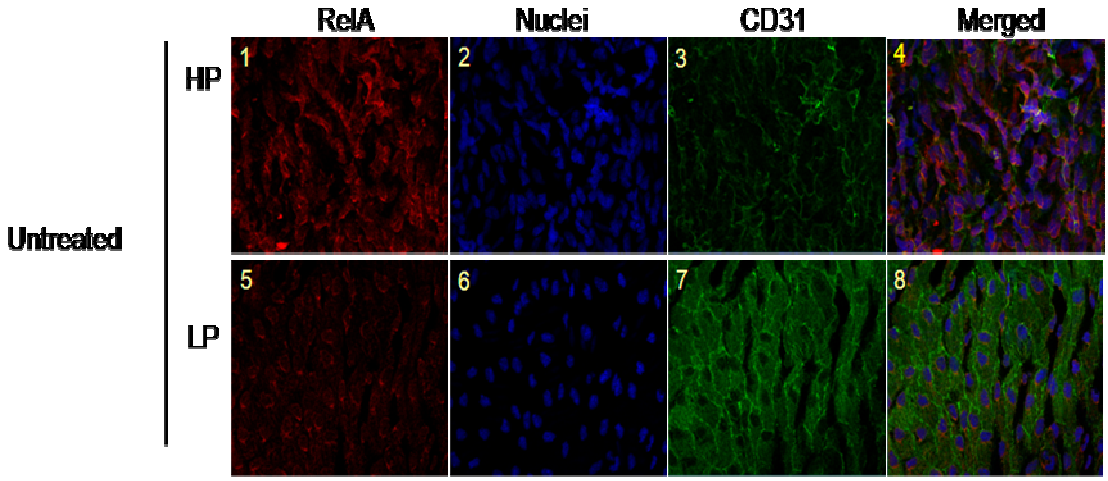

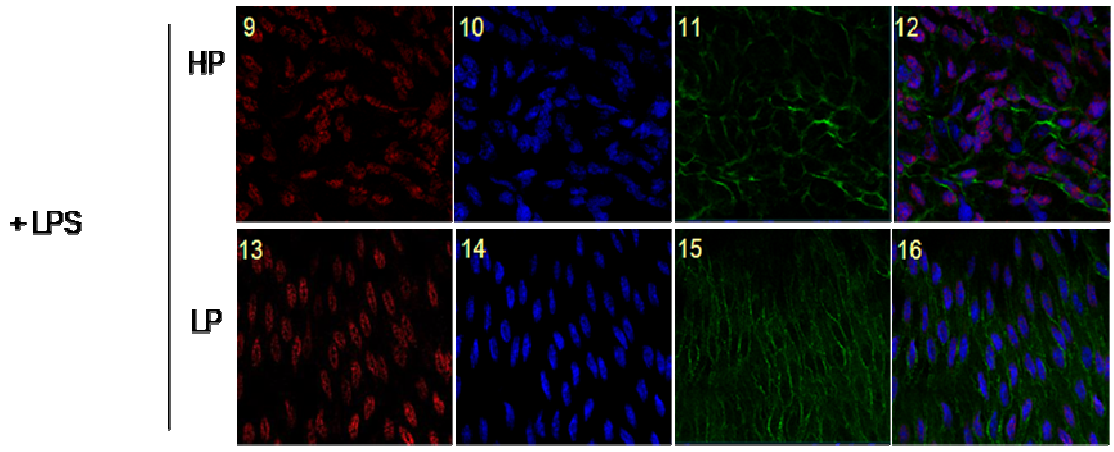

Fig 3.5 Assesment of RelA level in murine aortic endothelial cells.
C57BL/6 mice were injected with 50 µg LPS i.p. for 30 minutes (panels 9-16) or left untreated as controls (panels 1-8) (n=2 in each group). Aortae were fixed and then stained *en face* using anti-RelA primary antibodies and AlexaFluor 568-conjugated secondary antibodies (red). The endothelium was then stained using a 488-labelled anti-CD31 antibody (green). Nuclei were counterstained in all samples using 633-labelled DRAQ5 (blue). Fluorescence at the lumenal surface of HP and LP sites of the aortic arch was detected using confocal LSM. Representative images of HP and LP regions obtained from the same mouse are shown.

3.3.2 NF-κB transcriptional activity in HP and LP regions of murine aorta

Transgenic NF-κB luciferase reporter mice were used to assess the spatial distribution of NF-κB transcriptional activity in murine aortic endothelium *in vivo*. In particular, I focused on the HP and LP regions that were defined by the group of Myron Cybulsky (Iiyama *et al.*, 1999).

NF-κB-driven luciferase activity was very low in aortae from untreated animals (Figure 3.6 A, panel 1). LPS treatment elevated NF-κB activity in EC in the aortic arch and upper parts of the thoracic descending aorta (Figure 3.6 A, panels 2-5). Quantitative analysis also revealed that NF-κB was elevated to a greater extent in HP compared to LP regions (Figure 3.6 B). This indicates that EC in the HP region of the aortic arch are primed for enhanced NF-κB transcriptional activation in response to LPS.

A

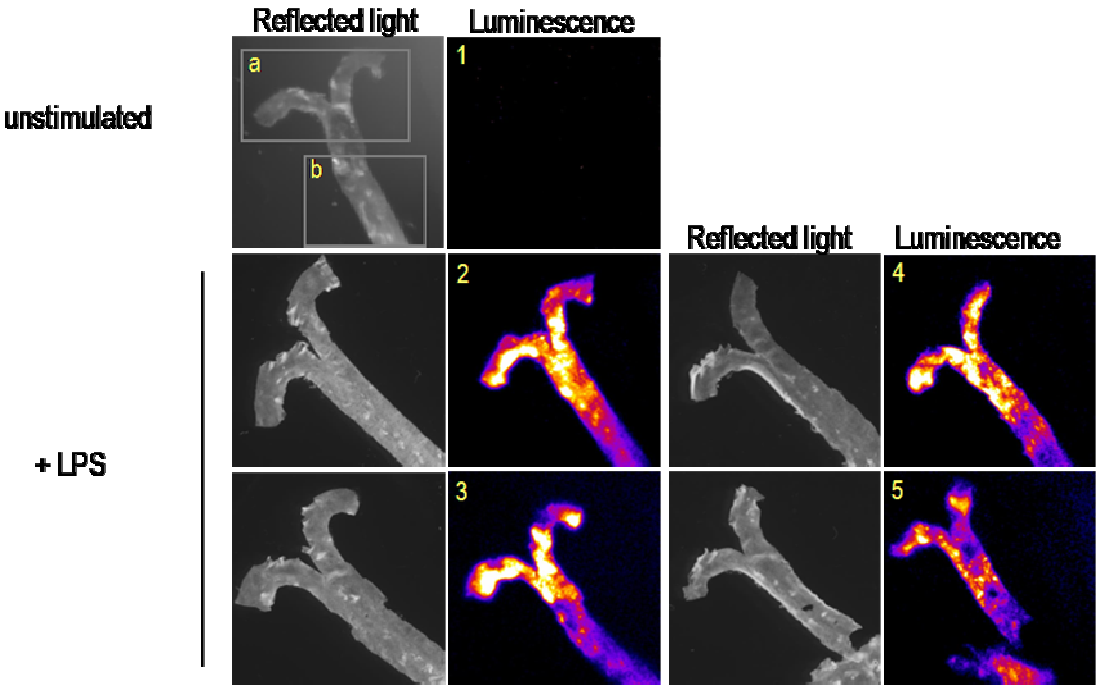

B

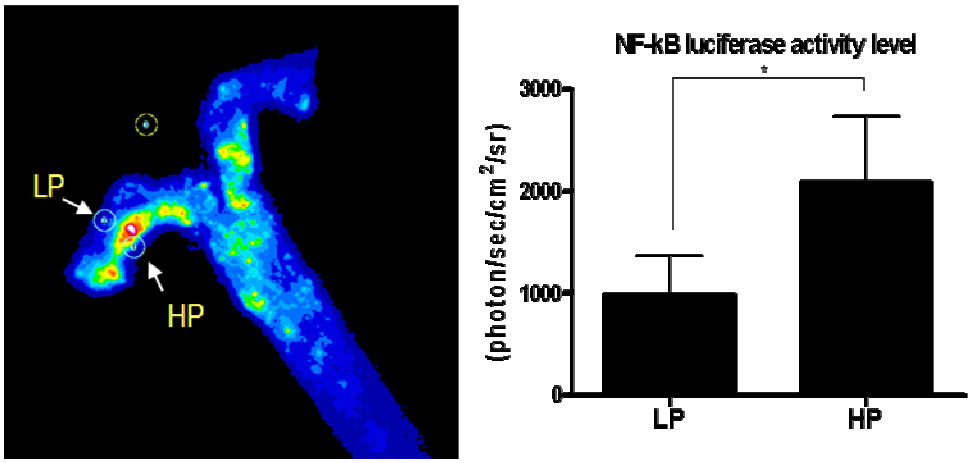

Fig 3.6 Constitutive and LPS-induced NF-κB transcriptional activity in the murine aortic endothelium.
(A) Transgenic NF-κB-luciferase mice were either left untreated (panel 1), or treated with 50 µg LPS i.p. for 4h (panels 2-5). Aortae were harvested, opened longitudinally and immersed in 1.5 mg/ml luciferin substrate in medium. Luciferase activity at endothelial surfaces was assessed by measuring luminescence at the lumenal side of the vessel (pseudocoloured). Reflected light images were obtained and are also shown. The arch and descending aorta are indicated with *a* and *b* respectively. (B) Luminescence intensity was measured at LP and HP sites of treated aortae (n=4). A representative image is shown with LP and HP sites indicated. Rates of photon detection are shown as means ±SD after subtracting background signals. Differences between samples were analyzed using a paired t-test (*p=0.0275). Note that EC in the HP region in the aortic arch possessed enhanced NF-κB activation in response to LPS.

3.3.3 NF-κB expression and activity at intercostal ostia

The intercostial ostias are branching sites of the aortic vessels, which can be seen as paired orifices along the aorta. These sites are exposed to abnormal hemodynamics and are susceptible to inflammation and atherosclerosis. In mice, an intimal "cushion" is found upstream of the orifice. The function of this cushion is uncertain, but it may influence mixing of blood to ensure sufficient blood supply to aortic branches. The intimal cushion consists of smooth muscle cells covered by an endothelial layer.

Spatial variation in NF-κB expression levels at intercostal ostia

We wanted to examine the expression of NF-κB/RelA in EC surrounding the ostia and to compare it with adjacent regions that are resistant to atherosclerosis and exposed to normal flow patterns

To investigate to which extent RelA is distributed in/around the ostia, we performed immunofluorescence staining in the descending aortae followed by confocal microscopy. Quantitative studies of 8 ostia revealed that RelA levels are elevated in EC that surrounded the intimal cushion compared to adjacent EC experiencing unidirectional laminar flow (Figure 3.7).

A

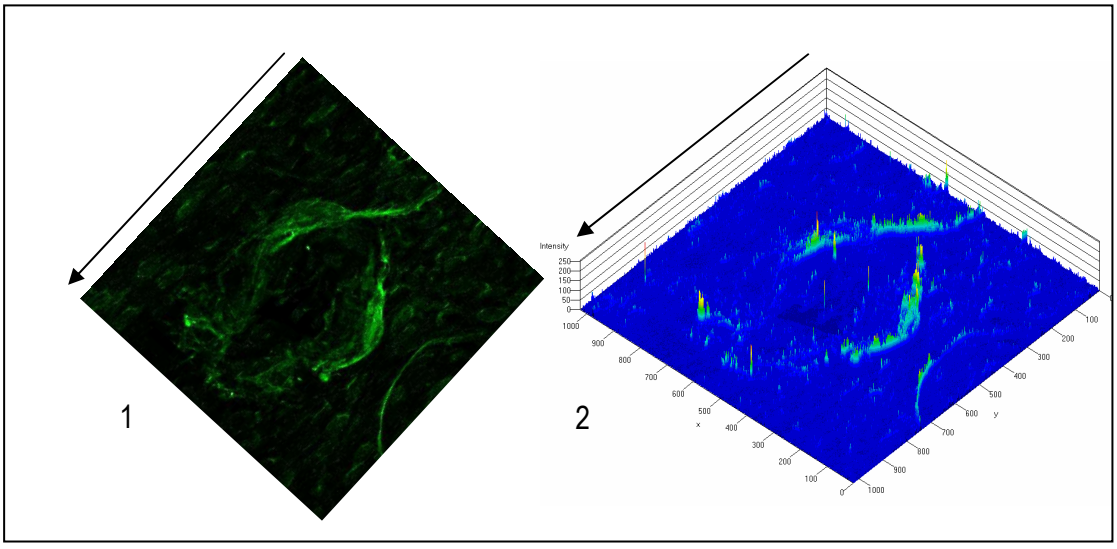

B

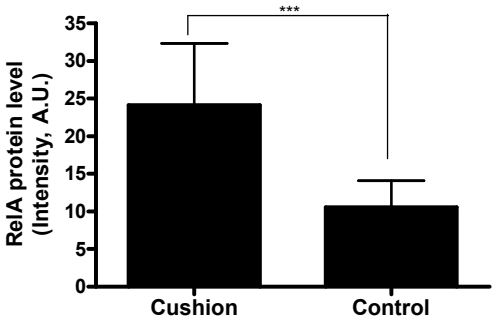

Figure 3.7 RelA distribution at intercostal ostias.
Aortae from untreated C57BL/6 (n=4) were fixed and then stained *en face* using anti-RelA primary antibodies and AlexaFluor 488-conjugated secondary antibodies (green). Fluorescence at ostia (n=8) was measured by making optical sections of the tissue using confocal LSM and rearranging images back into 3D projections. (A) (1) A single optical slice through an ostium is shown from the lumenal side of the descending aorta, (2) Pseudo3D images showing RelA staining intensity were obtained using the LSM software. The arrows show the direction of blood flow. (B) Fluorescence was quantified in 8 ostias for the intimal cushion and from adjacent areas exposed to laminar flow (Control). Data are shown as means ±SD. Differences between samples were analyzed using a paired t-test (***p=0.0003).

NF-κB luciferase activity in aorta at sites of disturbed flow

We have earlier seen that NF-κB transcriptional activity in transgenic NF-κB-reporter mice is enhanced at HP sites of the aortic arch in response to LPS. To assess if this is the same case with the intercostal ostia (which are also highly susceptible to atherosclerosis) we set up parallel experiments focusing on the descending aorta and ostia of intercostals arteries.

We could see that NF-κB activation in response to LPS was elevated in some of the intercostal ostias compared to adjacent regions (Figure 3.8 A and B). I conclude therefore that EC exposed to abnormal hemodynamics at the intercostal ostia contain elevated levels of NF-κB proteins and are primed for enhanced NF-κB activation in response to LPS.

A

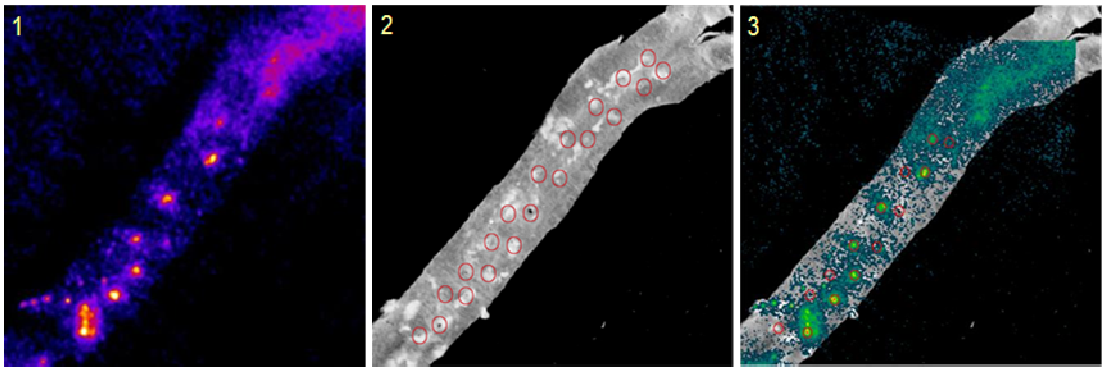

B

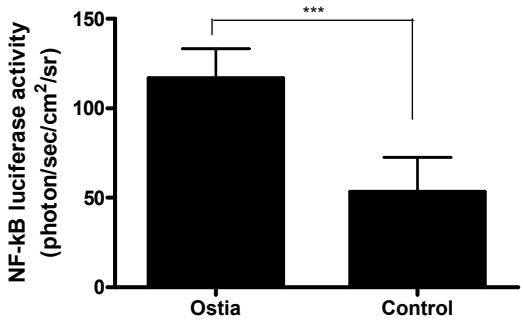

Figure 3.8 LPS-induced NF-κB transcriptional activity at areas exposed to disturbed and laminar flow.
(A) Transgenic NF-κB-luciferase mice (n=2) were treated with 50 µg LPS i.p. for 4h. Aortae were harvested, opened longitudinally and immersed in 1.5 mg/ml luciferin substrate in medium. Representative images are shown. Luciferase activity at endothelial surfaces was assessed by measuring luminescence at the lumenal side of the vessel (panel 1, pseudocoloured). Reflected light images of the aortae were obtained (panel 2), and overlaid with luminescence images to locate luminescence at intercostal ostias (panel 3). (B) Rates of photon detection at ostias and adjacent areas (Control) are shown as means ±SD. Differences between samples were analyzed using a paired t-test (*** $p<0.0001$). Note that EC at ostias possessed enhanced NF-κB activities compared to adjacent sites.

3.4 Expression of NF-κB target genes in atherosusceptible and atheroresistant regions of the aorta

The preliminary data from our lab revealed that pre-shearing had highly selective effects on transcriptional targets of TNFα, by suppressing pro-inflammatory transcripts but enhancing cytoprotective transcripts *in vitro* (Partridge *et al*., 2007). We wanted to investigate whether these findings could be valid *in vivo*, and to which extent the distribution of these transcripts in the murine aorta were correlated with NF-κB activity.

3.4.1 Spatial distribution of VCAM-1

As we can see in the unstimulated animals VCAM-1 was expressed at very low levels (Figure 3.9 A, panels 1-8; Figure 3.9 B). Upon LPS stimulation *in vivo,* VCAM-1 was significantly elevated in both HP and LP regions, but to a greater extent in HP regions (Figure 3.9 A, panels 9-16; Figure 3.9 B). These results indicate that VCAM-1 expression is tightly correlated with enhanced NF-κB activity in HP regions. We can therefore conclude that EC in the HP region are primed for pro-inflammatory activation.

A

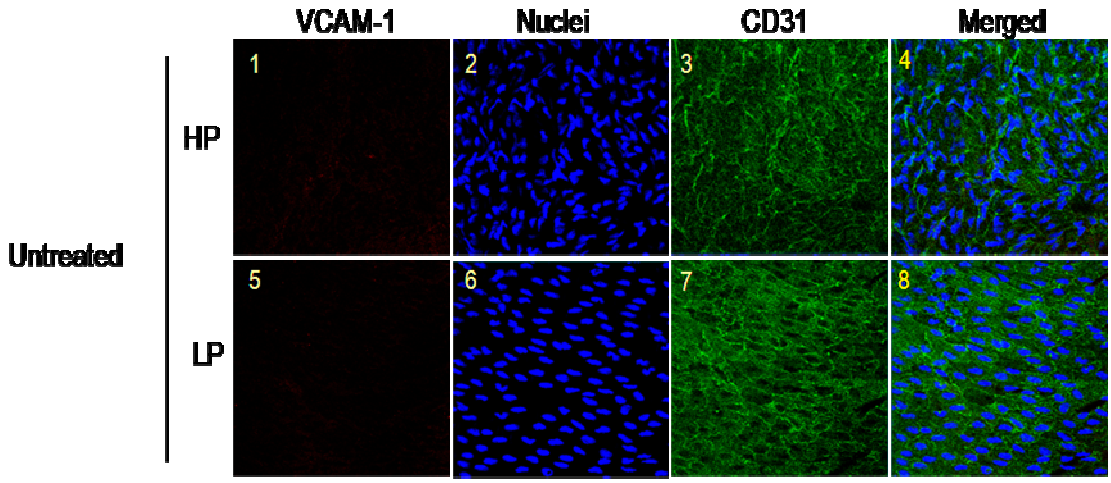

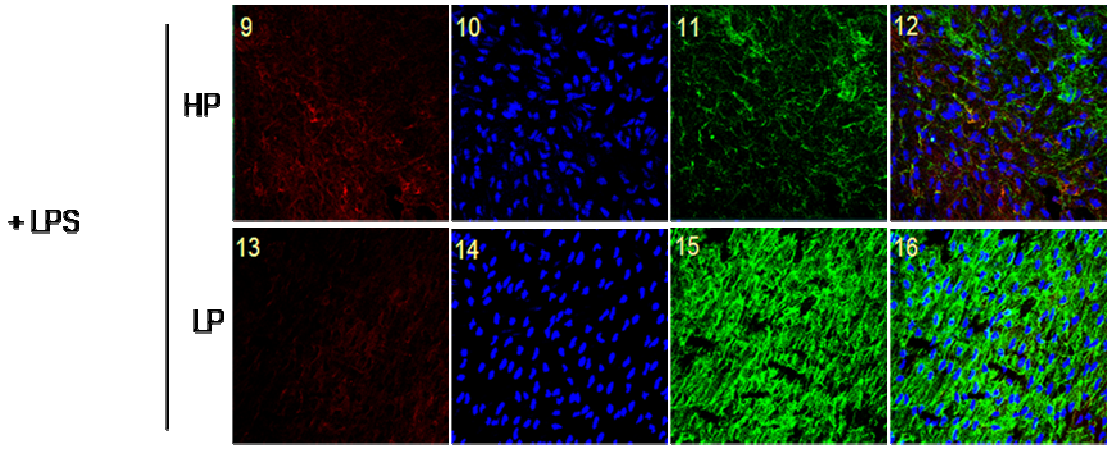

B

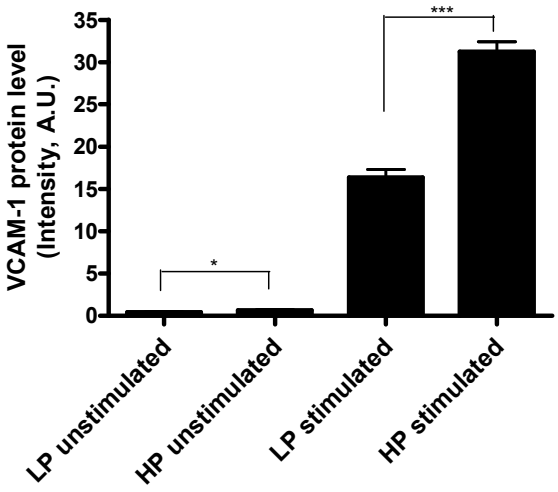

Fig 3.9 VCAM-1 expression in the aortic endothelium.
(A) C57BL/6 mice were injected with 50 µg LPS i.p. for 6h (panels 9-16) or remained untreated as controls (panels 1-8) (n=4 in each group). Aortae were fixed and then stained *en face* using anti-VCAM-1 primary antibodies and AlexaFluor 568-conjugated secondary antibodies (red). The endothelium was stained using a 488-labelled anti-CD31 antibody (green). Nuclei were counterstained in all samples using 633-labelled DRAQ5 (blue). Fluorescence at the lumenal surface of HP and LP sites of the aortic arch was detected using confocal LSM. Representative images of HP and LP regions obtained from the same mouse are shown. (B) Fluorescence was quantified in 100-150 cells randomly selected from 5-10 images of each area. Data are shown as means ±SEM. Differences between samples were analyzed using a paired t-test (*p=0.0162, ***p<0.0001). Endothelial cells expressed higher levels of VCAM-1 in response to LPS in HP than in LP areas of the aortic arch.

3.4.2 Distribution of A1 in the murine aorta

A1 is an anti-apoptotic Bcl-2 homologue that is known to be activated through the NF-κB route and induces cell viability. To assess the expression of A1 in the murine aorta in response to LPS we

performed a preliminary study in BXSB 1,4 mice which are prone to a lupus-like autoimmune syndrome (an excess of these animals were available in the unit).

This experiment showed that A1 has a low constitutive distribution (Figure 3.10 A, panels 1-8; Figure 3.10 B) and was induced modestly in response to LPS (Figure 3.10 A, panels 9-16; Figure 3.10 B). There was no significant difference in A1 expression in areas exposed to laminar or disturbed flow. These findings now need to be validated in a wild type mice strain (C57BL/6).

A

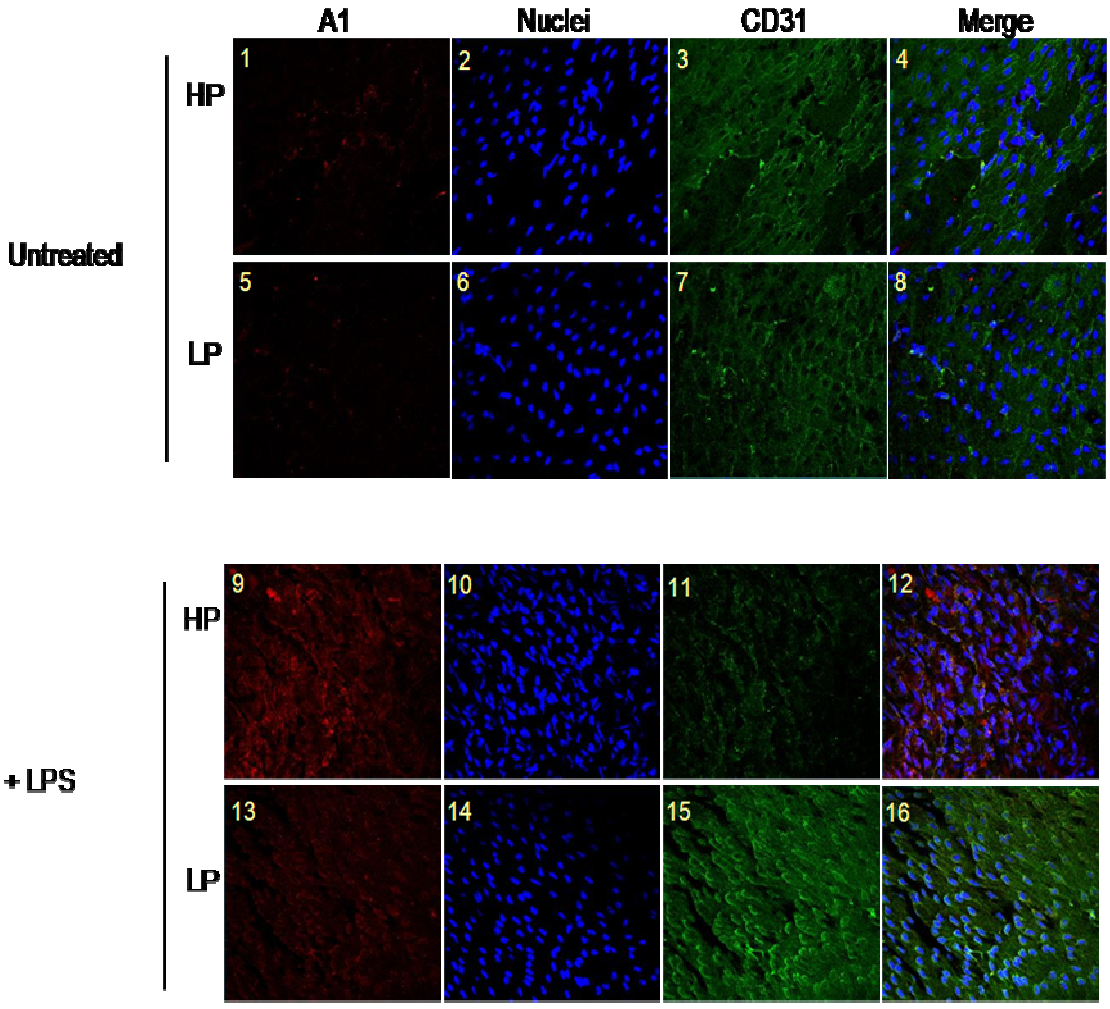

B

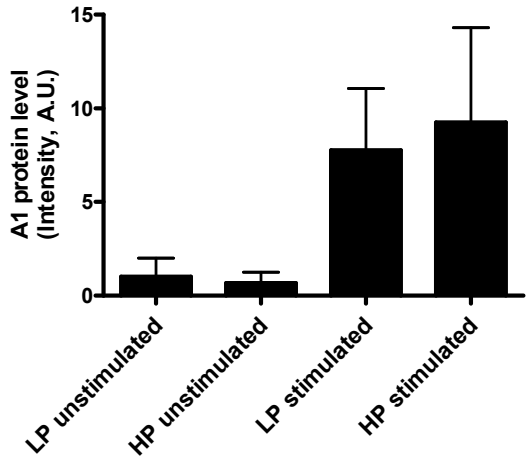

Figure 3.10 Spatial distribution of A1 in the murine aorta.
(A) BXSB 1,4 mice were injected with 50 µg LPS i.p. for 5h (panels 9-16) or left untreated as controls (panels 1-8) (n=2 in each group). Aortae were fixed and then stained *en face* using anti-A1 primary antibodies and AlexaFluor 568-conjugated secondary antibodies (red). The endothelium was stained using a 488-labelled anti-CD31 antibody (green). Nuclei were counterstained using 633-labelled DRAQ5 (blue) in all samples. Fluorescence at the lumenal surface of HP and LP sites of the aortic arch was detected using confocal LSM. Representative images of HP and LP regions obtained from the same mouse are shown. (B) Fluorescence was quantified in 100-150 cells randomly selected from 5-10 images of each area. Data are shown as means ±SEM. Differences between samples were analyzed using a paired t-test (ns). A1 experiences a modest up-regulation upon systemic stimulation of the immune system, and is distributed similarly in HP and LP areas of the aortic arch.

3.5 Spatial distribution of Nrf2 in areas exposed to disturbed and laminar flow

Recent studies have shown that Nrf2 is a critical transcription factor that regulates several genes contributing to important cellular defence mechanisms against the toxicity of electrophiles and ROS (Kobayashi & Yamamoto, 2005). It has also been shown that Nrf2 is regulated by laminar and oscillatory flow in human EC (Hosoya *et al*., 2005). We wanted to investigate whether Nrf2 is activated in atheroprotected regions in the mouse aorta.

3.5.1 Nrf2 expression and activity in atherosusceptible regions of the murine aorta

By confocal immunofluorescence microscopy we examined the constitutive Nrf2 protein levels in the murine aorta. Figure 3.11 show that Nrf2 expression is predominant in the HP region of the aortic arch (Figure 3.11 A, compare panels 1 and 5; Figure 3.11 B).

A

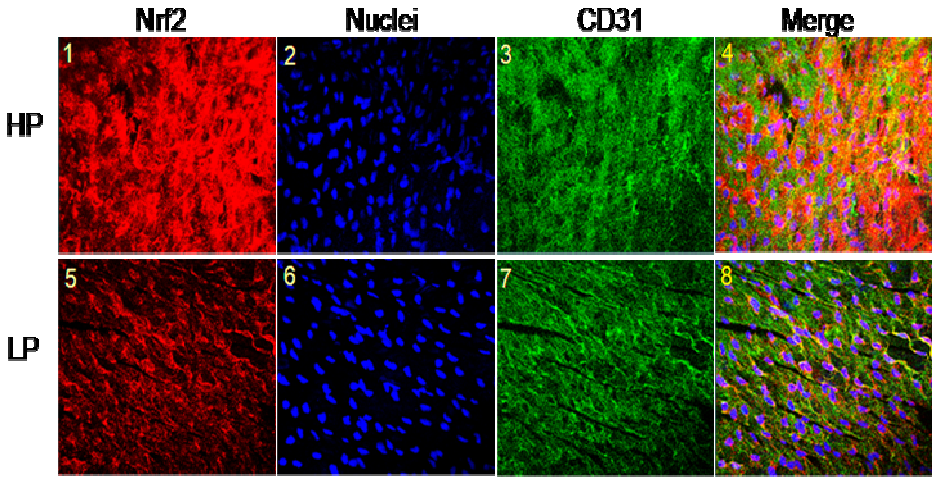

B

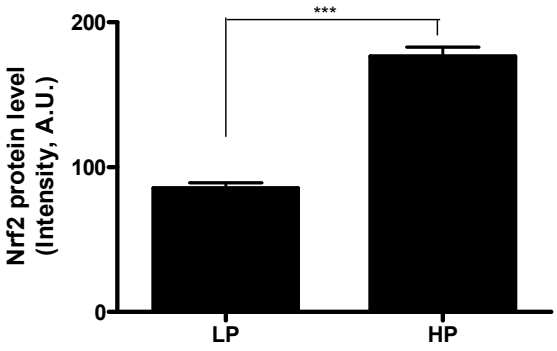

Figure 3.11 Spatial distribution of Nrf2 in the murine aorta.
(A) Aortae from C57BL/6 mice were fixed and then stained *en face* using anti-Nrf2 primary antibodies and AlexaFluor 568-conjugated secondary antibodies (red). The endothelium was stained using a 488-labelled anti-CD31 antibody (green). Nuclei were counterstained using 633-labelled DRAQ5 (blue). Fluorescence at the lumenal surface of HP and LP sites of the aortic arch was detected using confocal LSM. Representative images of HP and LP regions obtained from the same mouse are shown. (B) Fluorescence was quantified in 100-150 cells randomly selected from 5-10 images of each area. Data are shown as means ±SEM. Differences between samples were analyzed using a paired t-test (*p=0.0162, ***p<0.0001).

We were also interested in assessing whether Nrf2 was *activated* in regions exposed to atheroprotectice hemodynamic flow, as earlier shown by other groups (Dai *et al*., 2007). To do this we measured the nuclear/cytoplasmic ratio of Nrf2 in both HP and LP regions (note that Nrf2 enters the nucleus upon activation). As we can se in Figure 3.12, there were no significant differences in Nrf2 translocation between the two regions (Figure 3.12 B).

A

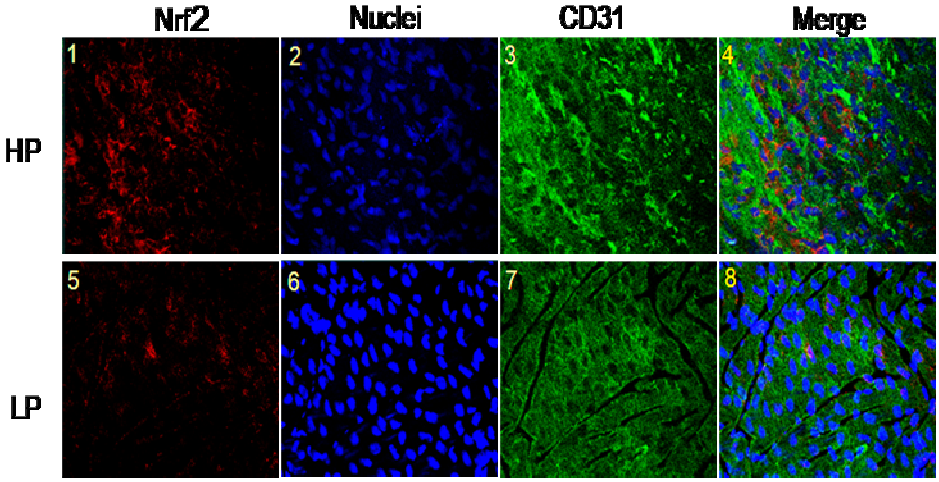

B

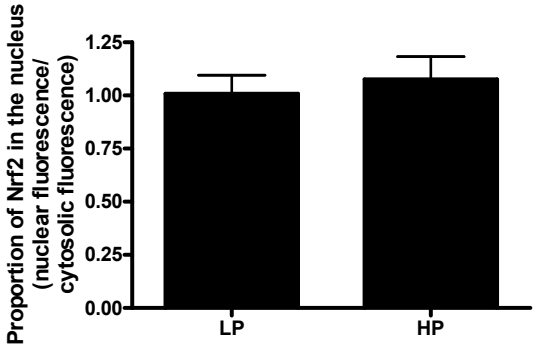

Figure 3.12 Nrf2 activity level at HP and LP sites of the aortic arch.
Aortae from untreated C57BL/6 mice (n=4) were harvested, fixed and then stained *en face* using anti-Nrf2 primary antibodies and AlexaFluor 568-conjugated secondary antibodies (red). The endothelium was stained using a 488-labelled anti-CD31 antibody (green). Nuclei were counterstained in all samples using 633-labelled DRAQ5 (blue). Fluorescence at the lumenal surface of HP and LP sites of the aortic arch was detected using

confocal LSM. The detector gain for the 568 channel was turned down at both sites for optimal visualization of cytoplasmic and nuclear compartments. (B) Fluorescence was quantified in 100-150 cells randomly selected from 5-10 images of each area. Data are shown as means ±SEM. Differences between samples were analyzed using a paired t-test (ns).

3.5.2 Nrf2 luciferase transcriptional activity in the murine aortic endothelium

To further investigate the expression of Nrf2 in the murine aorta, we looked at transgenic luciferase reporter mice. There was no distinct pattern of Nrf2 activities in the aorta and we observed similar Nrf2-luciferase activities in atherosusceptible (lesser curvature of aortic arch, ostia) and atheroresistant (greater curvature, descending thoracic aorta) regions (Figure 3.13 A, panels 1-4; Figure 3.13 C). It is plausible however that the resolution of this system is insufficient to identify potential differences between neighbouring cells. Thus immunostaining of aortae from Nrf2-luciferase animals using anti-luciferase antibodies should now be carried out to assess Nrf2 activity at a single cell resolution.

A **B**

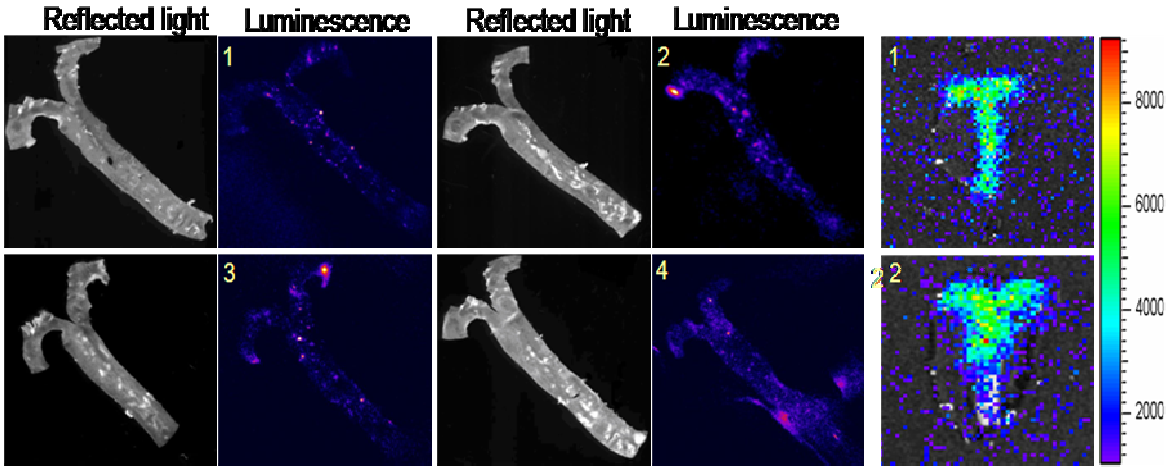

C

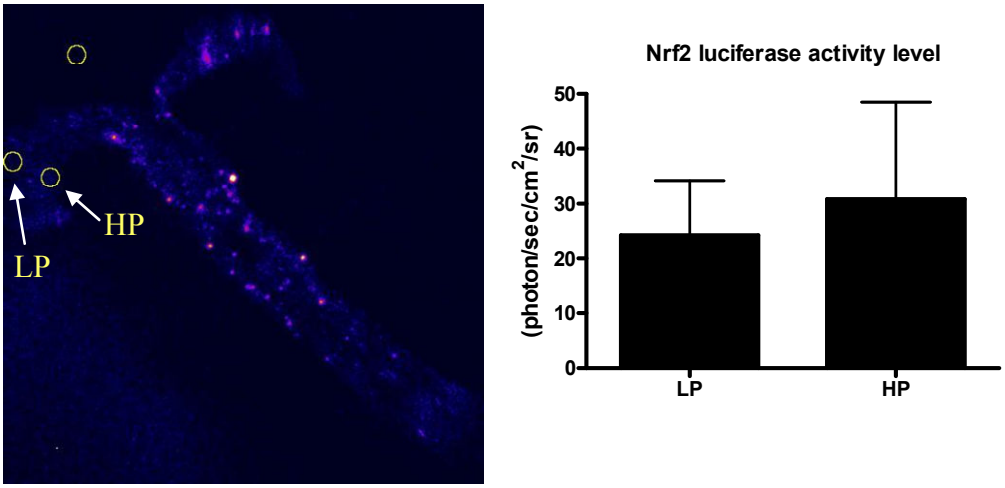

Fig 3.13 Constitutive Nrf2 transcriptional activity in the murine aortic endothelium.
(A) Aortae from transgenic Nrf2-luciferase mice (n=4) were harvested, opened longitudinally and immersed in 1.5 mg/ml luciferin substrate in medium. Luciferase activity at endothelial surfaces was assessed by measuring luminescence at the lumenal side of the vessel (pseudocoloured). Reflected light images were obtained and are also shown. (B) Luciferase activity was abolished in the endothelium by gentle scraping of the luminal side of the lower descending aorta. Images show aorta before (1) and after (2) scraping. (C) Luminescence intensity was measured at LP and HP sites. A representative image is shown. Rates of photon detection are shown as means ±SD after subtracting background signals. Differences between samples were analyzed using a paired t-test (ns). Note that endothelial cells in the HP region in the aortic arch show no increased Nrf2 transcriptional activity compared to LP region.

4 Discussion

4.1 Endothelial cell morphology in atherosusceptible and atheroresistant regions in the murine aorta

Endothelial cells, which line the vessel wall and regulate vascular homeostasis, are sensitive to shear stress which is a mechanical force generated at endothelial surfaces by flowing blood. One marker of endothelial dysfunction *in vivo* is the disorganization of cell shapes.

Our findings revealed that endothelial cells in a region of the aorta that is resistant to atherosclerosis (called LP for 'low probability') were elongated and organized in a parallel pattern to the direction of blood flow. Nuclei in this area were also well organized and appeared to be oval. Cultured EC are known to align themselves in response to shear stress, thus it is likely that EC in the LP region are orientated as a result of physiological responses to the hemodynamic flow pattern. In the HP region (high probability of atherosclerosis) where EC are exposed to low oscillatory shear, they possessed polygonal, irregular shapes and were randomly oriented relative to the direction of blood flow. The nuclei were also less organized than in the LP area.

Other investigators have also revealed that the endothelial cell morphology reflects the surrounding hemodynamic environment *in vivo* (Hajra *et al.,* 2001, Passerini *et al.,* 2004). I found that this morphology pattern was highly reproducible for the HP and LP region in the murine aorta. To a certain extent this was also used as a tool for confirming the correct identification of these regions in the aortic arch.

The mechanosensitive molecular mechanisms that determine shear stress-mediated endothelial shape change remain controversial. Still, a growing body of evidence supports an integrated signaling network in which cytoskeletal polymers transmit apical shear forces to membrane attachment sites at which conformational changes in associated proteins initiate signalling. During cell locomotion and shape change events, the actin cytoskeleton is remodelled extensively, primarily by adding and subtracting subunits at free filament ends. Cytoskeletal remodelling also occurs in response to fluid shear stress in endothelial cells. The effect of high shear streamlines the endothelial cell and reduces the peak shear stresses imposed on individual cells (Osborn *et al.,* 2006). Thus the characteristic elongated morphology of endothelial cells in atheroresistant sites exposed to high rates of unidirectional flow may result from cytoskeletal changes in response to shear stress.

4.2 Spatial distribution of NF-κB in the murine aorta

Current data implicate NF-κB as a key regulator of shear stress-induced inflammatory gene expression. The expression of NF-κB sub-units and pro-inflammatory proteins (e.g. VCAM-1, E-selectin) is elevated in atherosclerosis-prone regions before or in the absence of fatty streak formation, indicating that they may be very early events in the atherosclerotic progression (Nakashima *et al.,* 1998; Iiyama *et al.,* 1999; Wilson *et al.,* 2000). One of my aims was to establish whether there is a correlation between flow and NF-κB transcriptional activity *in vivo,* a subject that has not previously been investigated.

4.2.1 The NF-κB subunit RelA display increased expression and activity in athero-prone sites of the murine aorta

My findings revealed that RelA protein levels were significantly greater in the HP compared to the LP region in unstimulated murine aorta, thus supporting a previous study (Hajra *et al*., 2000). This

observation may be linked to the unique hemodynamic properties of these areas. The HP area, in which EC express high levels of RelA protein, is exposed to low hemodynamic shear. In contrast, EC in the LP region are exposed to protective, high shear and express low levels of RelA. Also, constitutive nuclear localization of RelA was significantly elevated in areas of low shear, hence suggesting but not proving that this region may be associated with increased NF-κB transcriptional activity. Collectively, these findings suggest that the HP area may be primed for NF-κB dependent pro-inflammatory activation. In contrast, the relatively low levels of RelA in the LP region would imply that NF-κB activity may be reduced in this area compared to the HP region.

By challenging endothelial cells with LPS for 30 minutes *in vivo*, I found a complete translocation of RelA to the nucleus in *both* HP and LP regions. This particular finding does not support Myron Cybulsky's group, who suggested that nuclear translocation of RelA exclusively in the HP region in response to LPS (Hajra *et al.,* 2000). Interestingly, this group conceded in their paper that the absence of RelA nuclear localization in LP regions in LPS-treated mice could have been due to an experimental artifact as low-level signal quantitation was diminished in their system. I conclude therefore that my observations may differ from those of Cybulsky due to the superior sensitivity of the immunostaining/confocal microscopy method that I used to measure RelA levels. I also concluded that NF-κB activity in the LP region therefore needs to be assessed in a more robust manner, specifically by using a high-sensitivity reporter system.

4.2.2 NF-κB transcriptional activity is elevated in HP vs. LP regions of the murine aorta in response to LPS

To assess directly the spatial distribution of NF-κB transcriptional activity in aortic endothelium, I used a transgenic strain of mice containing an NF-κB-luciferase reporter. Reporter gene systems are beneficial

in this setting because they are highly sensitive, amendable to quantitation and provide a direct measurement of transcriptional activity. Previously, transgenic reporter mice have successfully been used to investigate the eNOS promoter activity in vascular endothelium *in vivo* (Cheng *et al*., 2005).

By measuring endothelial luminescence in the aortic arch and the descending aorta, I found that NF-κB was activated by 4 hours of LPS in not only the HP, but also in the LP region of the aorta. I found a significant difference in these two regions, where NF- κB transcriptional activity was strongly induced in the HP region in contrast to the LP region. This indicates that endothelial cells in the HP region of the aortic arch are primed for enhanced NF-κB activation.

4.2.3 NF-κB activity is elevated in regions of the murine aorta exposed to abnormal hemodynamic flow

As earlier described, the intercostal ostia are areas of the descending aorta with disturbed, abnormal blood flow. The intimal cushion, which in part is responsible for these alterations in blood flow is situated upstream of the intercostal orifice. I examined this area in both untreated wild type mice and NF-κB-luciferase reporter mice challenged with LPS injections. My findings revealed that RelA levels are elevated at the intimal cushion compared to an adjacent area that experiences normal, laminar flow. NF-κB transcriptional activity was also elevated in this area, indicating that EC exposed to abnormal hemodynamics at the intercostal ostia may be primed for enhanced inflammatory activation in response to LPS.

These data are in part consistent with other investigators findings as the aortic branching sites are well-known to be susceptible to atherosclerotic lesion formation. In immature human aortae, it has been shown that lesions occur downstream of branch ostia. In contrast, at later ages lesions develop in a

more lateral or upstream distribution and are plausible to be caused by prolonged abnormalities in the hemodynamic environment. In mice, this pattern is to a greater extent inconsistent (McGillicuddy *et al.,* 2001). It would be interesting therefore to see whether NF-κB transcriptional activities at the aortic branch correspond to the elevated RelA protein level upstream of the ostia. This would demand an alternative strategy than can assess NF-κB activities at a single cell resolution e.g. through analysis of transgenic mice in which NF-κB drives GFP expression (this strain is currently under development in the Department of Nutrition, University of Oslo).

4.3 Expression of selected NF-κB target genes in atherosusceptible and atheroresistant regions of the murine aorta

To investigate the functional consequences of NF-κB activation in LP and HP sites of the murine aorta we evaluated the expression levels of VCAM-1 and A1, genes whose induced expression depends on NF-κB activation.

4.3.1 EC at atherosusceptible sites are primed for enhanced expression of the pro-inflammatory NF-κB target gene VCAM-1 in response to LPS

In the untreated aortic endothelium, I found that the constitutive levels of VCAM-1 are very low. At this level of fluorescence signal, the quantitation did dot reveal a highly significant difference between the HP and the LP regions. However, other groups have shown that VCAM-1 levels are elevated at atheroprone regions of the normal C57BL/6 mouse by using a more sensitive system that utilised quantum dot nanocrystals and two-photon excitation laser scanning microscopy (Ferrara *et al.,* 2005).

In contrast, by activating the endothelium with acute systemic stimuli for 6 hours, we could see that VCAM-1 expression levels were significantly increased throughout the aorta, but especially at the HP

region. A number of other investigators have studied the expression of VCAM-1 in murine aortae, and the findings are consistent with this study (Iiyama *et al.,* 1999; Nakashima *et al*., 1998).

If we compare this finding with the pattern we observed for the RelA/NF-κB expression, we can notice the similarities in the spatial distribution. This suggests that VCAM-1 activity is correlated to NF- κB transcriptional activity. Consequently, a strong correlation between nuclear translocation of RelA and the expression of pro-inflammatory transcripts is established.

4.3.2 Expression of the cytoprotective protein A1 is upregulated by LPS in the murine aorta

My findings revealed that the unstimulated aortic endothelium expressed very low levels of A1 protein. However, upon systemic acute activation by LPS, an increase in A1 protein was observed. The HP (exposed to low shear) and LP (high shear) regions did not show a significant difference in the expression of A1. These data are consistent with studies of cultured EC that demonstrated that the induction of A1 by pro-inflammatory stimuli is not regulated by shear stress (Duriez *et al*., 2000).

These findings on the expression of A1 were assessed in BXSB 1,4 mice and are not directly comparable with my other findings which were carried out in C57BL/6 mice. These data should therefore be looked at as preliminary findings which now need to be validated in a wild type strain of mice (BL/6). Unfortunately, time did not allow for me to do these final experiments before submitting the thesis, but will be finished by one of my co-workers within the Intracellular Signaling group.

4.3.3 NF-κB target genes are induced by LPS treatment

My studies suggest that the relatively high levels of NF-κB components in the HP region are functionally quite responsive, whereas the NF-κB signal transduction pathway in the LP region was largely

quiescent. Although we saw initial NF-κB activation of the LP region in response to LPS, this effect may therefore have been quickly repudiated. Differences in the expression of VCAM-1 and A1 may also reflect different sensitivities of the genes to NF-κB activation.

Theoretically, CD31 could be used as a control for the above experiments, because the expression of this protein is constitutive, not upregulated by LPS or cytokines and thought to be independent of NF-κB activation. We found that the efficiency of staining of CD31 was inconsistent between experiments. This may be due to incomplete antibody binding or other technical reasons. We decided therefore not to use CD31 staining as a negative control, but merely as an endothelial marker.

4.4 Does high shear stress mediate atheroprotective effects in aortic endothelium by activating Nrf2

Previously, the Nrf2/EpRE pathway has been identified as a system for antioxidant protection and suppression of redox-sensitive inflammatory genes (Chen *et al*., 2005). This suggests that targeting the Nrf2/EpRE pathway may represent a novel therapeutic approach for the treatment of inflammatory diseases such as atherosclerosis. Nrf2 activity in cultured EC can be upregulated by laminar flow, but the mechanism by which biomechanical forces induce Nrf2 activation is not well understood. It has previously been suggested that Nrf2 may be an important negative regulator of inflammation in arteries exposed to high shear e.g. the LP region.

In this study it was revealed that Nrf2 expression was more prevalent in the HP area of the aortic arch compared to the LP region. I also found that there was no difference in the extent of nuclear translocation in the HP or LP regions. Collectively, these data suggest that Nrf2 activation may be higher in the HP region than the LP region, which is the opposite of what we expected. Dai *et al.* have

recently suggested that Nrf2 is predominantly nuclear localized in the atherosclerosis-resistant region, whereas its localization is diffuse in the susceptible region (Dai *et al*., 2007). Similar findings have previously been shown in cultured endothelial cells (Hosoya *et al.,* 2005). My findings are therefore inconsistent with those of Dai *et al.* and further experiments will be required to address this.

To validate my findings, the specificity of the primary antibody I used in this experiment needs to be assessed. By examining antibody binding to the aortic endothelium in Nrf2 gene knockout mice we can assess whether the epitope binding is specific to Nrf2 or whether non-specific binding can occur.

I used an alternative technology employing transgenic mice containing an ARE/EpRE-luciferase reporter gene to further investigate Nrf2 activity in the murine aorta. Luminescence data showed a patchy distribution of Nrf2 activity that did not correlate with anatomical references of different flow patterns. Quantitation revealed that there were little or no differences in Nrf2 activity in the HP or LP region of the aortic arch. We were surprised by the low constitutive Nrf2 level in these aortae, since the immunofluorescence staining showed such high protein amounts. Thus, it would be interesting to investigate possible differences of neighbouring cells. To do this, we would need to assess Nrf2 activity at a single cell resolution by using anti-luciferase antibodies and fluorescence LSM.

4.5 Spatial distribution of NF-κB activity in the aorta and its relevance in atherosclerosis

The most important finding of my study was that the NF-κB signal transduction pathway in endothelium of atherosusceptible regions was primed for enhanced responses to systemic activation stimuli. Thus lipopolysaccharide treatment resulted in NF-κB activation and up-regulated expression of NF-κB inducible genes predominantly in EC of the HP region.

One may speculate whether the NF-κB signal transduction pathway is upregulated or chronically activated in HP regions or downregulated in LP regions. Chronic exposure to laminar shear stress may upregulate the expression of unique genes such as Nrf2 that are atheroprotective, or may promote other mechanisms that actively repress expression of broad category of genes. Several groups have demonstrated that alterations in fluid dynamics induced by surgery to modify the geometry of vessels in conjunction with hypercholesterolemia can influence atherosclerotic lesion formation (Fishman et al 1975, Booth et al 1989), which further supports the role of hemodynamics in lesion development. Given the findings presented in this thesis, it would be very interesting to investigate whether such alterations in fluid dynamics can also alter the expression of NF-κB subunits, NF-κB transcriptional activity and pro-inflammatory activation *in vivo*, factors that are central regulators of the atherogenic process.

5 Conclusion

In this study I sought to investigate the correlation between atherosclerosis, hemodynamic flow patterns and the NF-κB signal transduction pathway. I found that the expression of RelA NF-κB subunits and NF-κB transcriptional activity was elevated in regions of the aortic endothelium exposed to low, oscillatory shear (HP region, ostia). I also demonstrated that the NF-κB-dependent pro-inflammatory molecule VCAM-1 was significantly increased in the HP region in response to systemic activation stimulus. In contrast, the anti-apoptotic, cytoprotective protein A1 was elevated in both HP and LP regions on encounter with LPS. The distribution of Nrf2 expression and activity did not vary between high shear and low shear regions, thus alternative studies will be required to fully assess the potential role of this transcription factor in atheroprotection.

Collectively, my findings suggest that murine aortic endothelial cells exposed to low shear stress are primed for enhanced NF-κB activation which drives pro-inflammatory activation, whereas endothelium in an environment of laminar unidirectional flow is protected. We can therefore conclude that the NF-κB pathway may have a prominent role in the initiation and progression of atherosclerotic lesions, and may serve as a target for novel therapies to prevent and treat atherosclerosis.

6 References

Alcamo, E., Alcamo, E., Mizgerd, J.P., Horwitz, B.H., Bronson, R., Beg, A.A., Scott, M., Doerschuk, C.M., Hynes, R.O., Baltimore, D. (2001). "Targeted mutation of TNF receptor 1 rescues the RelA deficient mouse and reveals a critical role for NF-κB in leukocyte recruitment." *J. Immunol.*167: 1592-1600.

Bisgrove, B.W., Yost, H.J. (2006). "The roles of cilia in developmental disorders and disease." *Development.* 133: 4131–4143.

Bonizzi, G., Karin, M. (2004). "The two NF-κB activation pathways and their role in innate and adaptive immunity." *Trends Immunol.* 25(6): 280-8.

Booth, R.F.G., Martin, J.F., Honey, A.C., Hassall, D.G., Beesley, J.E., Moncada, S. (1989). "Rapid development of atherosclerotic lesions in the rabbit carotid artery induced by perivascular manipulation." *Atherosclerosis*. 76: 257–268.

Brand, K., Page, S., Rogler, G., Bartsch, A., Brandl, R., Knuechel, R., Page, M., Kaltschmidt, C., Baeuerle, P.A., Neumeier, D. (1996) "Activated transcription factor nuclear factor-kappa B is present in the atherosclerotic lesion." *J. Clin. Invest.* 97(7): 1715-22.

Chen, X.L., Dodd, G., Thomas, S., Zhang, X., Wasserman, M.A., Rovin, B., Kunsch, C. (2006). "Activation of Nrf2/ARE pathway protects endothelial cells from oxidant injury and inhibits inflammatory gene expression." *Am. J. Physiol. Heart Circ. Physiol.* 290(5): H1862-70.

Chen, X.L., Kunsch, C. (2004). "Induction of cytoprotective genes through Nrf2/antioxidant response element pathway: a new therapeutic approach for the treatment of inflammatory diseases." *Curr. Pharm. Des.* 10: 879-891.

Chen, X.L., Varner, S.E., Rao, A.S., Grey, J.Y., Thomas, S., Cook, K., Wasserman, M.A., Medford, R.M., Jaiswal, A.K., Kunsch, C. (2003). "Laminar flow induction of antioxidant response element-mediated genes in endothelial cells. A novel anti-inflammatory mechanism." *J. Biol. Chem.* 278: 703-711.

Cheng, C., van Haperen, R., de Waard, M., van Damme, L.C.A., Tempel, D., Hanemaaijer, L., van Cappellen, G.W.A., Bos, J., Slager, C.J., Duncker, D.J., van der Steen, A.F.W., de Crom, R., and Krams, R. (2005). "Shear stress affects the intracellular distribution of eNOS: direct demonstration by a novel in vivo technique." *Blood.* 106: 3691–3698.

Chiu, J.J., Lee, P.L., Chen, C.N., Lee, C.I., Chang, S.F., Chen, L.J., Lien, S.C., Ko, Y.C., Usami, S., Chien, S. (2004). "Shear stress increases ICAM-1 and decreases VCAM-1 and E-selectin expressions induced by tumor necrosis factor-alpha in endothelial cells." *Arterioscl. Thromb. Vasc. Biol.* 24: 73–79.

Clinton, S., Underwood, R., Sherman, M., Kufe, D., Libby, P. (1992). "Macrophage-colony stimulating factor gene expression in vascular cells and in experimental and human atherosclerosis." *Am. J. Pathol.* 140**:** 301–316.

Collins, T., Cybulsky, M. (2001). "NF-κB: Pivotal mediator of innocent bystander in atherogenesis?" *J. Clin. Invest.* 107(3): 255-64.

Cybulsky, M.I., Iiyama, K., Li, H., Zhu, S., Chen, M., Iiyama, M., Davis, V., Gutierrez-Ramos, J.C., Connelly, P.W., Milstone, D.S. (2001). "A major role for VCAM-1, but not ICAM-1, in early atherosclerosis." *J. Clin. Invest.* 107(10): 1255-62.

Dai, G.H., Kaazempur-Mofrad, M.R., Natarajan, S., Zhang, Y.Z., Vaughn, S., Blackman, B.R., Kamm, R.D., Garcia-Cardena, G., and Gimbrone, M.A. (2004). "Distinct endothelial phenotypes evoked by arterial waveforms derived from atherosclerosis-susceptible and -resistant regions of human vasculature." *Proc. Nat. Acad. Sci. USA.* 101: 14871–14876.

Dai, G.H., Vaughn, S., Zhang, Y., Wang E.T., Guillermo, G.C., Gimbrone, M.A. (2007). "Biomechanical forces in atherosclerosis-resistant vascular regions regulate endothelial redox-balance via Phosphoinositol 3-kinase/Akt-dependent activation of Nrf2." *Circ. Res.* 101: 723-733.

Davies, P.F. (2007). "Hemodynamics in the determination of the endothelial phenotype and flow mechanotransduction. In: 'Endothelial Biomedicine; A Comprehensive Treatise.", Ed. Aird, W.C. *Cambridge University Press.* 220-235.

De Smaele, E., Zazzeroni, F., Papa, S., Nguyen, D.U., Jin, R.G., Jones, J., Cong, R., Franzoso, G. (2001). "Induction of gadd45beta by NF-kappa B downregulates pro-apoptotic JNK signalling." *Nature.* 414: 308–313.

Dimmeler, S., Assmus, B., Hermann, C., Haendeler, J., Zeiher, A.M. (1998). "Fluid shear stress stimulates phosphorylation of Akt in human endothelial cells - Involvement in suppression of apoptosis." *Circ. Res.* 83: 334-341.

Dimmeler, S., Haendeler, J., Rippmann, V., Nehls, M., Zeiher, A.M. (1996). "Shear stress inhibits apoptosis of human endothelial cells." *FEBS Lett.* 399: 71-74.

Dimmeler, S., Hermann, C., Galle, J., Zeiher, A.M. (1999). "Upregulation of superoxide dismutase and nitric oxide synthase mediates the apoptosis-suppressive effects of shear stress on endothelial cells." *Arterioscl. Thromb. Vasc. Biol*. 19: 656-664.

Duriez, P.J., Wong, F., Dorovini-Zis, K., Shahidi, R., Karsan, A. (2000). "A1 functions at the mitochondria to delay endothelial apoptosis in response to tumor necrosis factor." *J. Biol. Chem.* 275: 18099–18107.

Evans, P.C. (2005). "Regulation of pro-inflammatory signalling networks by ubiquitin: identification of novel targets for anti-inflammatory drugs." *Expert Rev. Mol. Med.* 7(12): 1-19.

Ferrara, D.E., Weiss, D.,Carnell, P.H., Vito, R.P., Vega, D., Gao, X., Nie, S., Taylor, W.R. (2006). "Quantitative 3D fluorescence technique for the analysis of en face preparations of arterial walls using quantum dot nanocrystals and two-photon excitation laser scanning microscopy." *Am. J. Physiol. Regul. Integr. Comp. Physiol.* 290: R114–R123.

Fishman, J.A., Ryan, G.B., Karnovsky, M..J. (1975). "Endothelial regeneration in the rat carotid artery and the significance of endothelial denudation in the pathogenesis of myointimal thickening." *Lab. Invest*. 32: 339–351.

Ghosh, S., May, M.J., Kopp, E.B. (1998). "NF-κB and Rel proteins: evolutionary conserved mediators of immune responses." *Annu. Rev. Immunol.* 16: 225-260.

Grabowski, E.F., Reininger, A.J., Petteruti, P.G., Tsukurov, O., Orkin, R.W. (2001). "Shear stress decreases endothelial cell tissue factor activity by augmenting secretion of tissue factor pathway inhibitor." *Arterioscl. Thromb. Vasc. Biol*. 21: 157-162.

Gu, L., Okada, Y., Clinton, S.K., Gerard, C., Sukhova, G.K., Libby, P., Rollins, B.J. (1998). "Absence of monocyte chemoattractant protein-1 reduces atherosclerosis in low-density lipoprotein-deficient mice." *Mol. Cell.* 2: 275–281.

Hajra, L., Evans, A.I., Chen, M., Hyduk, S.J., Collins, T., Cybulsky, M. I. (2000). "The NF-kappa B signal transduction pathway in aortic endothelial cells is primed for activation in regions predisposed to atherosclerotic lesion formation." *Proc. Nat. Acad. Sci. USA.* 97:9052–9057.

Haskard, D.O., (2004). "Accelerated atherosclerosis in inflammatory rheumatic diseses." *Scand. J. Rheumatol. 33: 281-292.*

Hayden, M.S., Ghosh, S. (2004). "Signaling to NF-kappa B." *Genes Dev*. 18: 2195–2224.

Helderman, F., Segers, D., de Crom, R., Hierck, B.P., Poelmann, R., Evans, P.C., Krams, R. (2007). "Effect of shear stress on vascular inflammation and plaque development." *Curr. Opin. Lipidol.* 18: 527–533.

Henke, N., Schmidt-Ullrich, R., Dechend, R., Park, J.K., Qadri, F., Wellner, M., Obst, M., Gross, V., Dietz, R., Luft, F.C., Scheidereit, C., Muller, D.N. (2007). "Vascular endothelial cell-specific NF-kappaB suppression attenuates hypertension-induced renal damage." *Circ. Res. 101(3): 268-76.*

Hermann, C., Zeiher, A.M., Dimmeler, S. (1997). "Shear stress induced up-regulation of superoxide dismutase inhibits tumor necrosis factor alpha-mediated apoptosis of endothelial cells." *Circulation.* 96: 2732.

Hockenbery, D., Nunez, G., Milliman, C., Schreiber, R.D., Korsmeyer, S.J. (1990). "Bcl-2 is an inner mitochondrial membrane protein that blocks programmed cell death." *Nature.* 348: 334.

Hosoya, T., Maruyama, A., Kang, M.I., Kawanati, Y., Shibitas, T., Uchidas, K., Itoh, K., Yamamoto, M. (2005). "Differential responses of the Nrf2/Keap1 system to laminar and oscillatory shear stresses in endothelial cells." *J. Biol. Chem.* 280(29): 27244-27250.

Huo, Y., and Ley, K. (2001). "Adhesion molecules and atherogenesis. *Act. Physiol. Scand.* 173: 35–43.

Iiyama, K., Hajra, L., Iiyama, M., Li, H.M., DiChiara, M., Medoff, B.D., Cybulsky, M.I. (1999). "Patterns of vascular cell adhesion molecule-1 and intercellular adhesion molecule-1 expression in rabbit and mouse atherosclerotic lesions and at sites predisposed to lesion formation." *Circ. Res.* 85: 199–207.

Iomini, C., Tejada, K., Mo, W., Vaananen, H., Piperno, G. (2004). "Primary cilia of human endothelial cells disassemble under laminar shear stress." *J. Cell. Biol.* 164: 811–817.

Jin, X., Mitsumata, M., Yamane, T., Yoshida, Y. (2002). "Induction of human inhibitor of apoptosis protein-2 by shear stress in endothelial cells." *FEBS Lett.* 529: 286-292.

Kadl, A., Leitinger, N. (2005). "The role of Endothelial cells in the Resolution of Acute Inflammation." *Antiox. Redox. Signal.* 7: 1744-1754.

Kobayashi, M., Yamamoto, M. (2005). "Molecular mechanisms activating the Nrf2-Keap1 pathway of antioxidant gene regulation." *Antioxid. Redox. Signal.* 7: 385-394.

Kol, A., Libby, P. (1998). "The mechanisms by which infectious agents may contribute to atherosclerosis and its clinical manifestations." *Trends Cardiovasc. Med.* 8(5): 191-9.

Ley, K., Huo, Y. (2001). "VCAM-1 is critical in atherosclerosis." *J. Clin. Invest.* 107(10): 1209-10.

Libby, P. (2002). "Inflammation in atherosclerosis." *Nature.* 420: 868–874.

Libby, P., Ridker, P. M., Maseri, A. (2002). "Inflammation and atherosclerosis." *Circulation.* 105: 1135–1143.

Lin, K., Hsu, P.P., Chen, B.P., Yuan, S., Usami, S., Shyy, J.Y., Li, Y.S., Chien, S. (2000). "Molecular mechanism of endothelial growth arrest by laminar shear stress." *Proc. Nat. Acad. Sci. USA.* 97: 9385-9389.

Mach, F., Sauty, A., Iarossi, A.S., Sukhova, G.K., Neote, K., Libby, P., Luster, A.D. (1999). "Differential expression of three T lymphocyte-activating CXC chemokines by human atheroma-associated cells." *J. Clin. Invest.* 104: 1041–1050.

Malek, A., Alper, S., Izumo, S. (1999). "Hemodynamic shear stress and its role in atherosclerosis." *JAMA.* 282: 2035-2042.

McGillicuddy, C.J., Carrier, M.J., Weinberg, P.D., (2001). "Distribution of lipid deposits around aortic branches of mice lacking LDL receptors and Apolipoprotein E." *Arterioscler.Thromb. Vasc. Biol.* 21: 1220-1225.

Monaghan, P., Robertson, D., Amos, T.A.S., Dyer, M.J.S., Mason, D.Y., Greaves, M.F. (1992). "Ultrastructural localization of Bcl-1 protein." *J. Histochem. Cytochem.* 40: 1819.

Motomiya, M., Karino, T. (1984). "Flow patterns in the human carotid artery bifurcation." *Stroke.*15(1): 50-6.

Nakashima, Y., Raines, E.W., Plump, A.S., Breslow, J.L., Ross, R. (1998). "Upregulation of VCAM-1 and ICAM-1 at atherosclerosis-prone sites on the endothelium in the ApoE-deficient mouse." *Arterioscler. Thromb. Vasc. Biol.* 18(5): 842-51.

Netea, M.G., van Deuren, M., Kullberg, B.J., Cavaillon, J.M., Van der Meer, J.W. (2002). "Does the shape of lipid A determine the interaction of LPS with Toll-like receptors?" *Trends Immunol*. 23(3): 135-9.

O'Brien, K.D., Allen, M.D., McDonald, T.O., Chait, A., Harlan, J.M., Fishbein, D., McCarty, J., Ferguson, M., Hudkins, K., Benjamin, C.D. (1993). "Vascular cell adhesion molecule-1 is expressed in human coronary atherosclerotic plaques. Implications for the mode of progression of advanced coronary atherosclerosis." *J. Clin. Invest.* 92(2): 945-51.

Osborn, E.A., Rabodzey, A., Dewey, C.F. Jr., Hartwig, J.H. (2006). "Endothelial actin cytoskeleton remodeling during mechanostimulation with fluid shear stress." *Am. J. Physiol. Cell Physiol.* 290: C444–C452.

Partridge, J., Carlsen, H., Enesa, K., Chaudhury, H., Zakkar, M., Luong, L., Kinderlerer, A., Johns, M., Blomhoff, R., Mason, J.C., Haskard, D.O., Evans, P.C. (2007). "Laminar shear stress acts as a switch to regulate divergent functions of NF-κB in endothelial cells." *FASEB J.* [Epub ahead of print]

Passerini, A.G., Polacek, D.C., Shi, C., Francesco, N.M., Manduchi, E., Grant, G.R., Pritchard, W.F., Powell, S., Chang, G.Y., Stoeckert, C.J., Davies, P.F. (2003). "Coexisting proinflammatory and antioxidative endothelial transcription profiles in a disturbed flow region of the adult porcine aorta." *Proc. Nat. Acad. Sci. USA.* 101(8): 2482-2487.

Resnick, N., Yahav, H., Shay-Salit, A., Shushy, M., Schubert, S., Zilberman, L.C., Wofovitz, E. (2003). "Fluid shear stress and the vascular endothelium:for better and for worse." *Prog. Biophys. Mol. Biol.* 81: 177-199.

Ross, R., Harker, L. (1976). "Hyperlipidemia and atherosclerosis." *Science.* 193: 1094–1100.

Satir, P., Christensen, S.T. (2007). "Overview of structure and function of mammalian cilia." *Annu. Rev. Physiol.* 69: 377–400.

Senftleben, U., Karin, M. (2002). "The IKK/NF-κB pathway." *Crit. Care Med.* 301: 18-26.

Sheikh, S., Rahman, M., Gale, Z., Luu, N.T., Stone, P.C.W., Matharu, N.M., Rainger, G.E.L., Nash, G.B. (2005). "Differing mechanisms of leukocyte recruitment and sensitivity to conditioning by shear stress for endothelial cells treated with tumour necrosis factor-alpha or interleukin-1 beta." *Brit. J. Pharmacol.* 145: 1052–1061

Sheikh, S., Rainger, G.E., Gale, Z., Rahman, M., Nash, G.B. (2003). "Exposure to fluid shear stress modulates the ability of endothelial cells to recruit neutrophils in response to tumor necrosis factor-alpha: a basis for local variations in vascular sensitivity to inflammation." *Blood.* 102: 2828–2834.

Stoneman, V.E.A., Bennett, M.R. (2004). "Role of apoptosis in atherosclerosis and its therapeutic implications." *Clinical Science.* 107: 343-354.

Taba, Y., Miyagi, M., Miwa, Y., Inoue, H., Takahashi-Yanaga, F., Morimoto, S., Sasaguri, T. (2003). "15-deoxy-delta 12,14-prostaglandin J2 and laminar fluid shear stress stabilize c-IAP1 in vascular endothelial cells." *Am. J. Physiol. Heart Circ. Physiol.* 285(1): H38-46.

Traub, O., Berk, B. (1998). "Laminar shear stress:mechanisms by which endothelial cells transducer an atheroprotective force." Arterioscler. *Thromb.* 18: 677-685.

Tzima, E., Irani-Tehrani, M., Kiosses, W.B., Dejana, E., Schultz, D.A., Engelhardt, B., Cao, G.Y., DeLisser, H., Schwartz, M. A. (2005). "A mechanosensory complex that mediates the endothelial cell response to fluid shear stress." *Nature.* 437: 426–431.

Van Antwerp, D.J., Martin, S.J., Verma, I.M., Green, D.R. (1998). "Inhibition of TNF-induced apoptosis by NF-kappa B." *Trends Cell. Biol.* 8(3): 107-11.

Van der Heiden, K., Groenendijk, B.C., Hierck, B.P., Hogers, B., Koerten, H.K., Mommaas, A.M., Gittenberger-de Groot, A.C., Poelmann, R.E. (2006). "Monocilia on chicken embryonic endocardium in low shear stress areas." *Dev. Dyn.* 235: 19–28.

Wilson, S.H., Caplice, N.M., Simari, R.D., Holmes, D.R. Jr, Carlson, P.J., Lerman, A. (2000). "Activated nuclear factor-kappaB is present in the coronary vasculature in experimental hypercholesterolemia." *Atherosclerosis.* 148(1): 23-30.

Wong, G.H.W., Elwell, J.H., Oberley, L.W., Goeddel, D.V. (1989). "Manganous superoxide-dismutase is essential for cellular-resistance to cyto-toxicity of tumor necrosis factor." *Cell.* 58: 923–931.

Yamawaki, H., Lehoux, S., and Berk, B.C. (2003). "Chronic physiological shear stress inhibits tumor necrosis factor-induced proinflammatory responses in rabbit aorta perfused ex vivo." *Circulation.* 108: 1619–1625.

Zarins, C.K., Giddens, D.P., Bharadvaj, B.K., Sottiurai, V.S., Mabon, R.F., Glagov, S., (1983). "Carotid bifurcation atherosclerosis:quantitative correlation of plaque localization with flow, velocity profiles and wall shear stress." *Circ. Res.* 53: 502-514.

Zong, W.X., Edelstein, L.C., Chen, C.L., Bash, J., Gelinas, C. (1999). "The prosurvival Bcl-2 homolog Bfl-1/A1 is a directtranscriptional target of NF-kappa B that blocks TNF alphainduced apoptosis." *Genes Dev*. 13: 382–387.

Internet references

1) http://www.who.int/cardiovascular_diseases/en/
2) http://www.irishhealth.com
3) http://bme.virginia.edu/ley/
4) http://opa.faseb.org/pdf/porro.pdf
5) http://www.zeiss.com
6) http://probes.invitrogen.com/resources/spectraviewer/